Electronic Supplementary Material (ESI) for Journal of Materials Chemistry C.

Supplementary information

Influence of mechanical, thermal, and electrical perturbations on the dielectric behaviour of guest-encapsulated HKUST-1 crystals

*Arun Singh Babal and Jin-Chong Tan**

Multifunctional Materials and Composites (MMC) Laboratory,

Department of Engineering Science, University of Oxford,

Parks Road, Oxford, OX1 3PJ, U.K.

* jin-chong.tan@eng.ox.ac.uk

Contents

1. Morphological and topological studies on HKUST-1 MOF powder and pellets

1.1 Particle size measurement

1.1.1 Scanning electron microscopy (SEM)

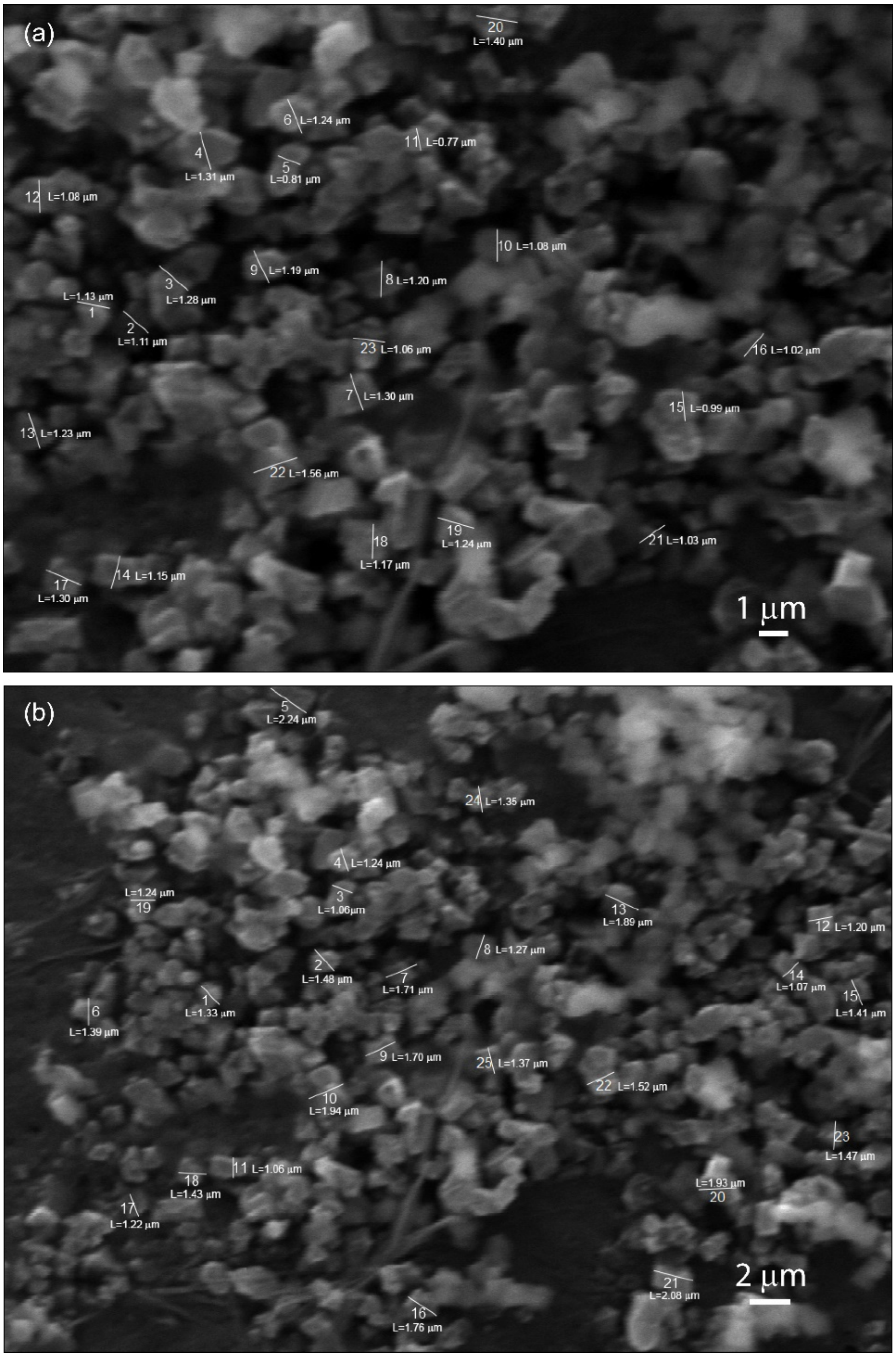

Figure S1: Measurement of total 50 individual particles of HKUST-1-S from the SEM images. The averaged particle size is 1.5 ± 0.74 μm.

1.1.2 Atomic force microscopy (AFM)

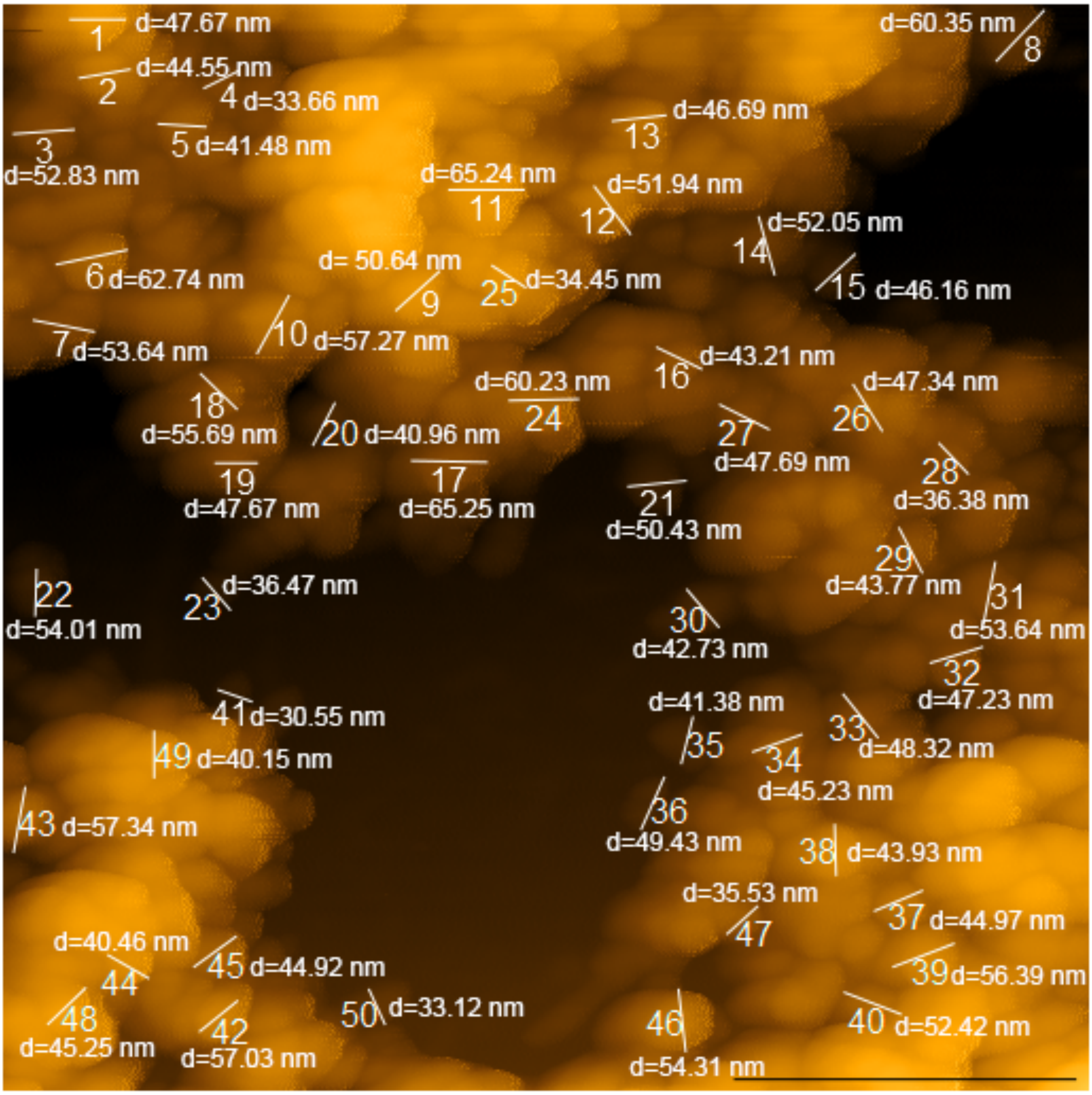

Figure S2: Measurement of total 50 individual particles of HKUST-1-S from the AFM image. The averaged particle size is 47.89 ± 17.36 nm.

2. Fourier transform Infrared spectroscopy (FTIR) of pressure pellets

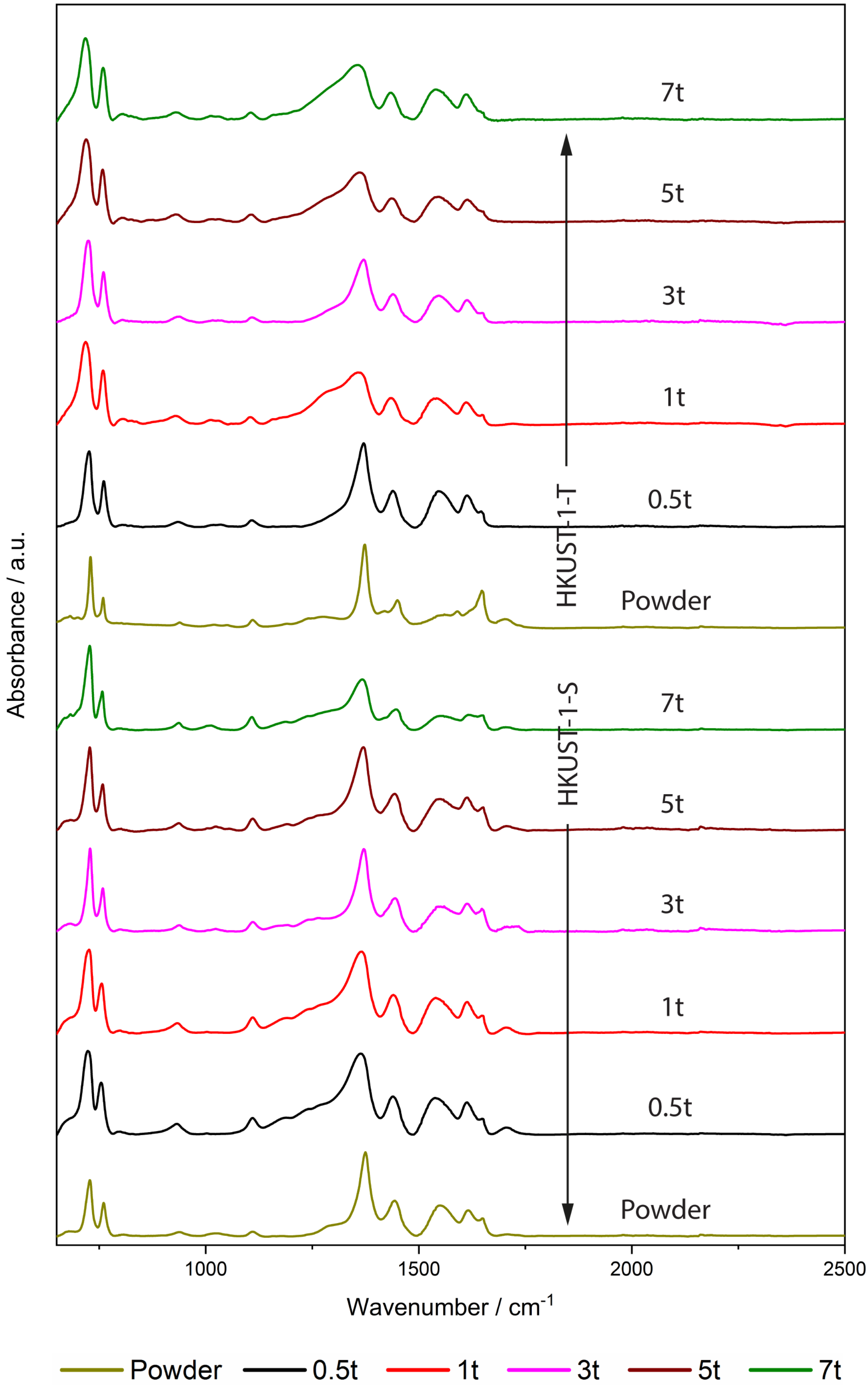

Figure S3: Normalized FTIR spectra of different type of HKUST-1-S and HKUST-1-T MOF pressure pellets.

3. Effect of pelleting pressure on FWHM (Full width at half maximum) value of the characteristic XRD peak

(a)

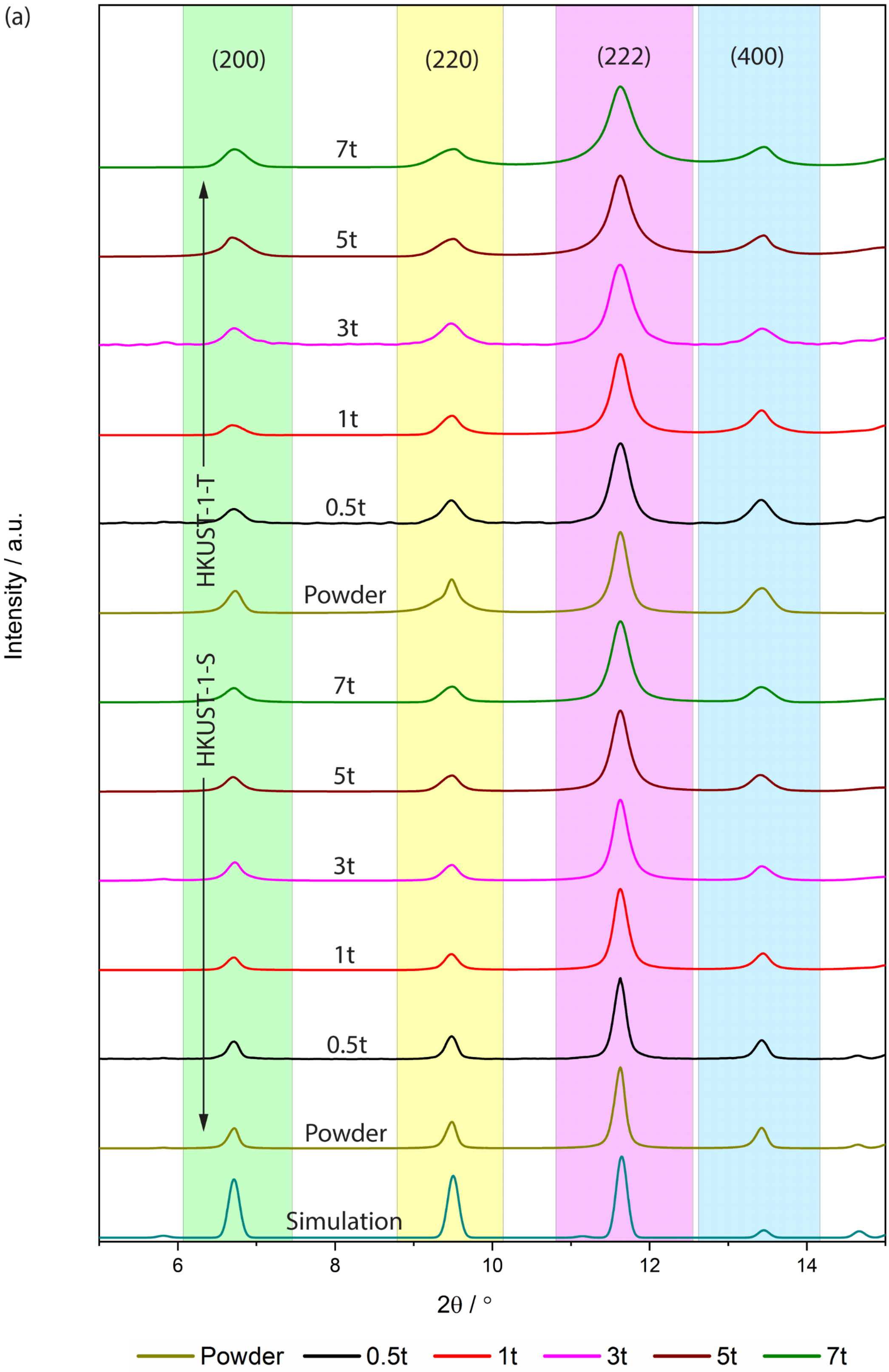

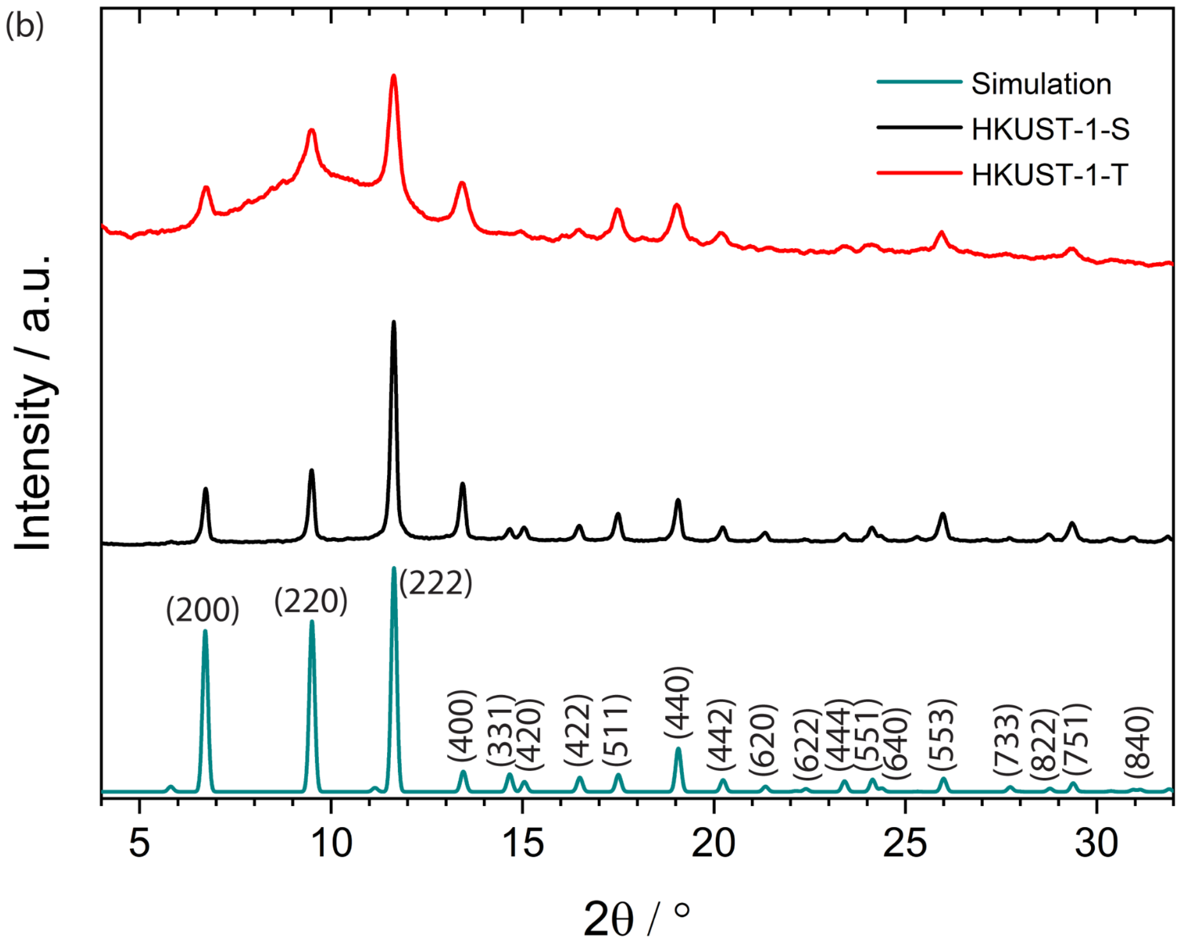

Figure S4: (a) XRD patterns of the HKUST-1 pellets prepared under a compressive force of 0.5t to 7t. (b) Comparison of the simulated XRD pattern of HKUST-1 with the as-synthesized powders of HKUST-1-S and HKUST-1-T (both without background subtraction), normalized to the (222) peak which has the highest intensity. HKUST-1-T exhibits a broad peak from 2θ of ~6° to 14° that superimpose the sharp Bragg peaks in the same region, thereby suggesting the presence of some semi-crystalline or amorphous products.

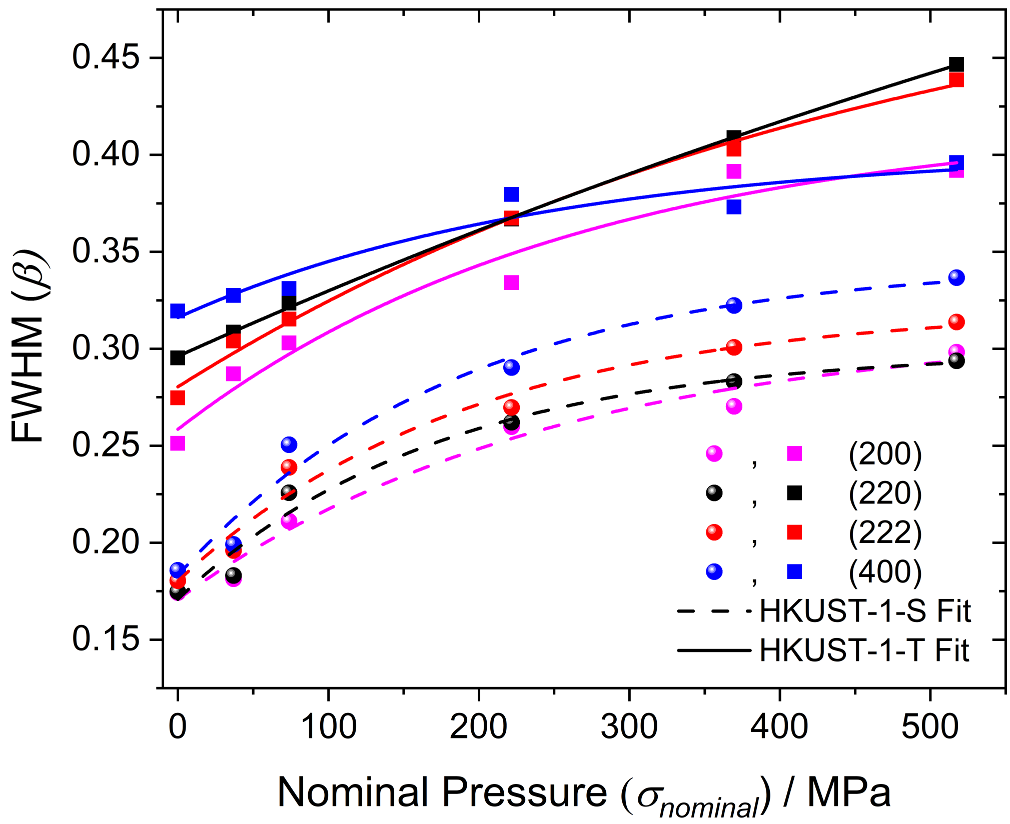

Figure S5: FWHM *vs* pelleting pressure plot for HKUST-1-S and HKUST-1-T samples.

4. N_2 Adsorption-desorption and thermal stability of HKUST-1 samples

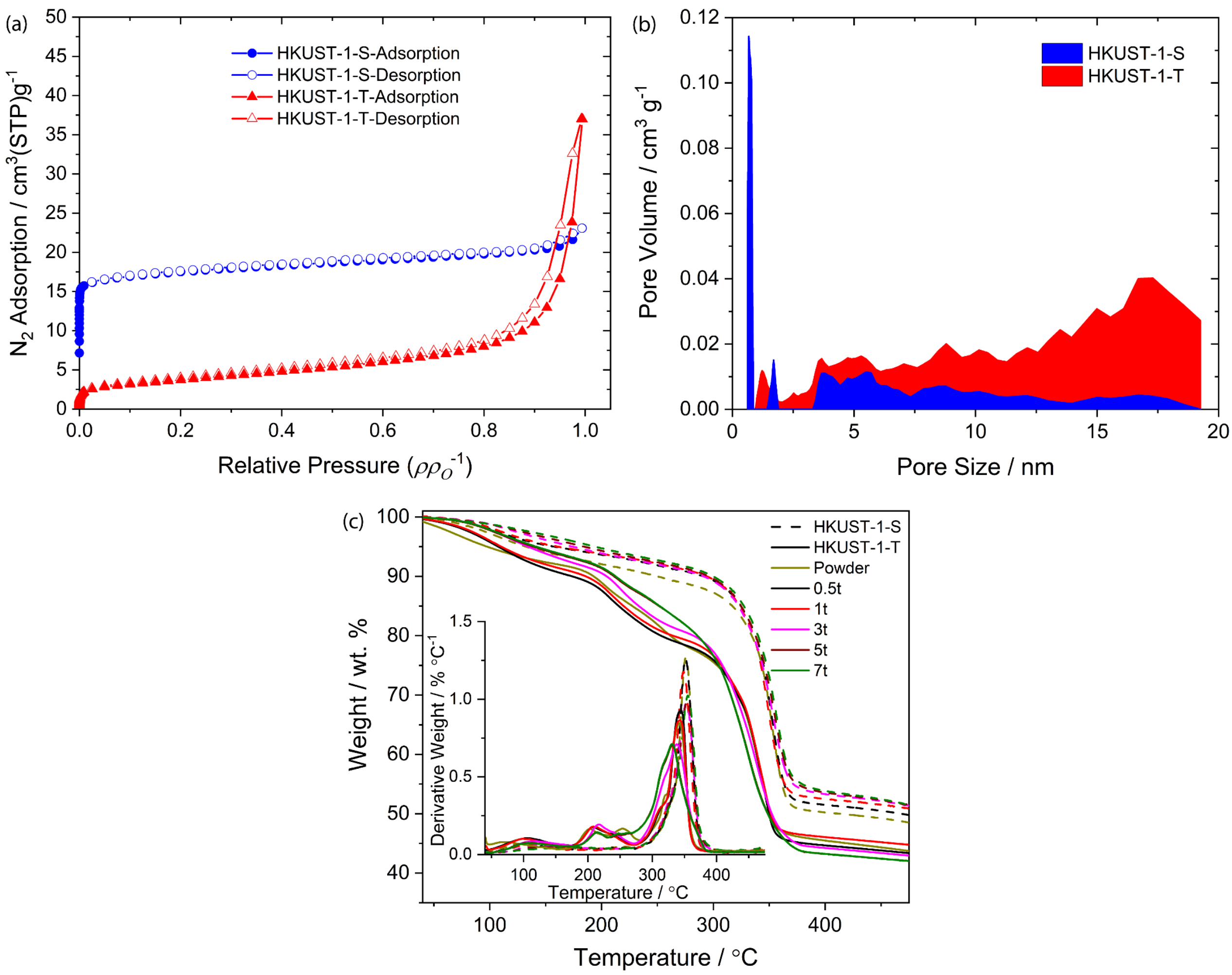

Figure S6: (a) Nitrogen adsorption-desorption isotherms of powder samples of HKUST-1-S (blue) and HKUST-1-T (red) at 77 K. The BET surface areas of the HKUST-1-S and HKUST-1-T samples are 1007 m²/g and 165 m²/g, respectively. (b) Pore size distributions determined from non-linear DFT model, assuming a combination of slit-shape and cylindrical-shape pores typically applied in MOF analysis. HKUST-1-S has predominantly micropores of < 2 nm, whereas HKUST-1-T is comprising mesopores from *ca.* 2-20 nm. (c) Thermo-gravimetric analysis plot of HKUST-1 samples as a function of temperature. The hump in the derivative plot suggests the presence of NEt_3 molecules resulted in $[Cu_3(BTC)_2].1.5N(CH_2CH_3)_3$.

5. Optical microscopy for pellet roughness measurements

5.1 HKUST-1-S pellets

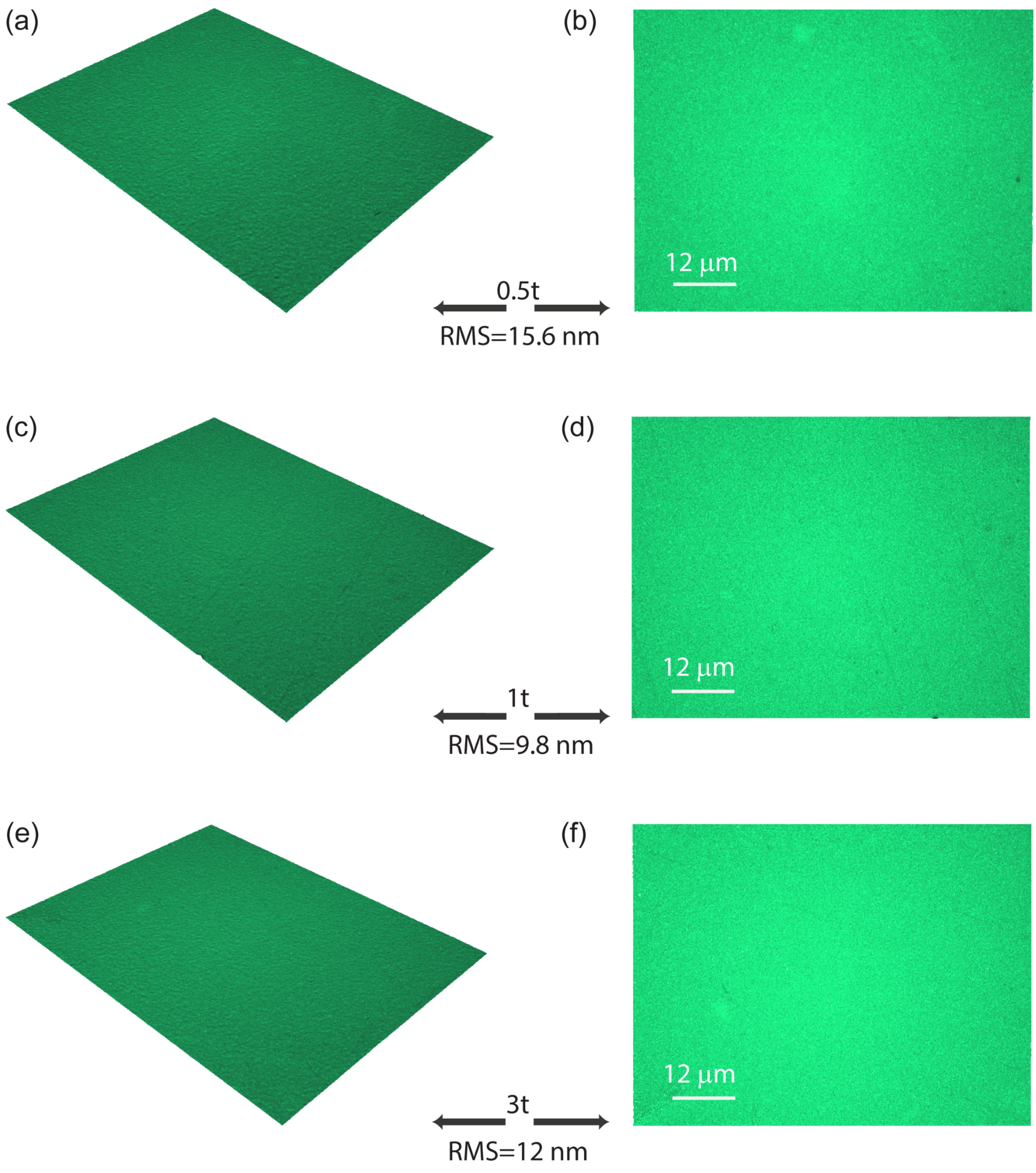

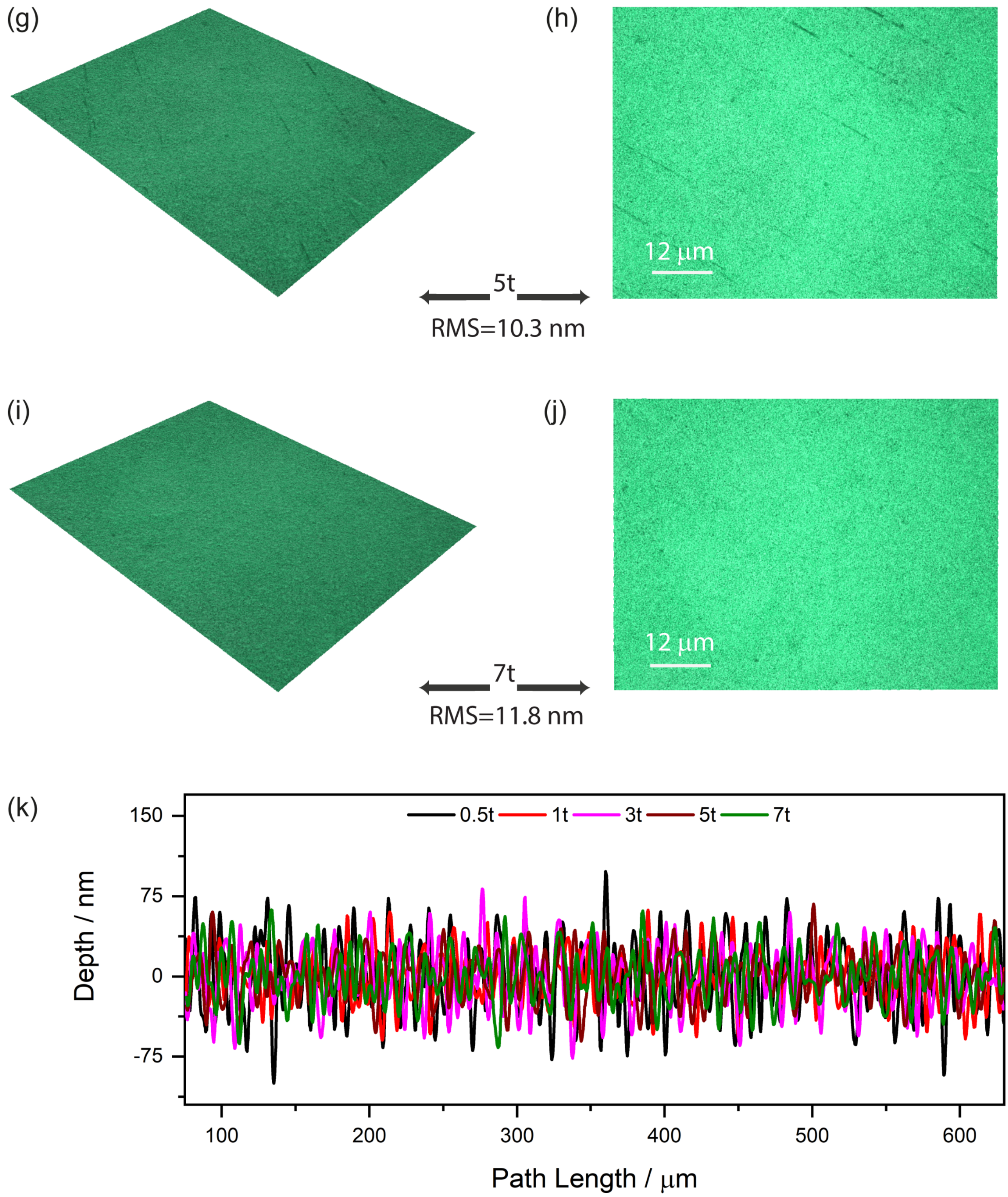

Figure S7: HKUST-1-S pellet surface roughness characterization using Alicona Infinite Focus Microscope at 20× optical magnification: (a)-(b) 0.5 ton, (c)-(d) 1 ton, (e)-(f) 3 ton, (g)-(h) 5 ton, (i)-(j) 7 ton, (k) pellet roughness profile by using the profile line width of 80 µm, respectively. (RMS=Root mean square roughness of profile)

5.2 HKUST-1-T pelletS

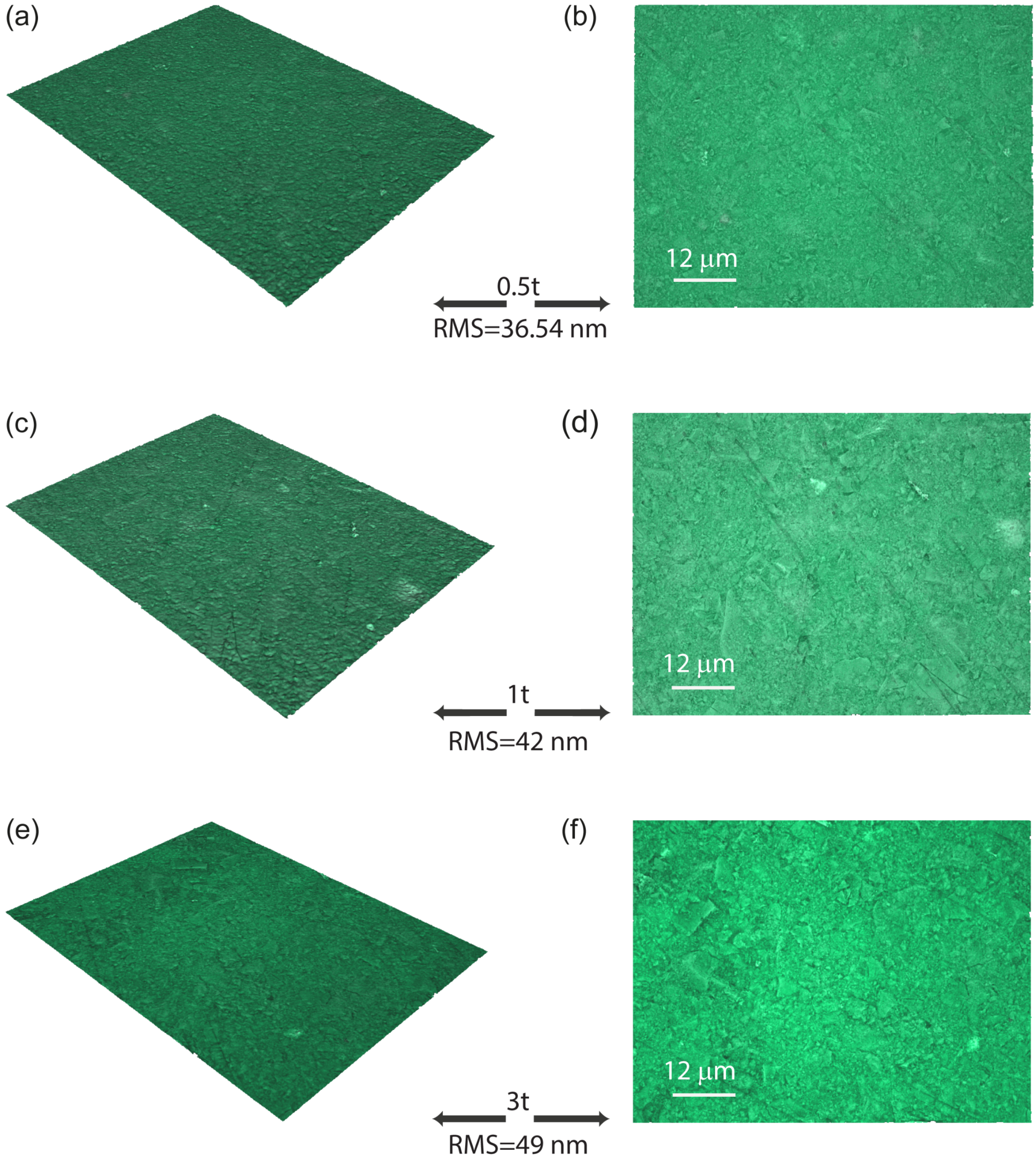

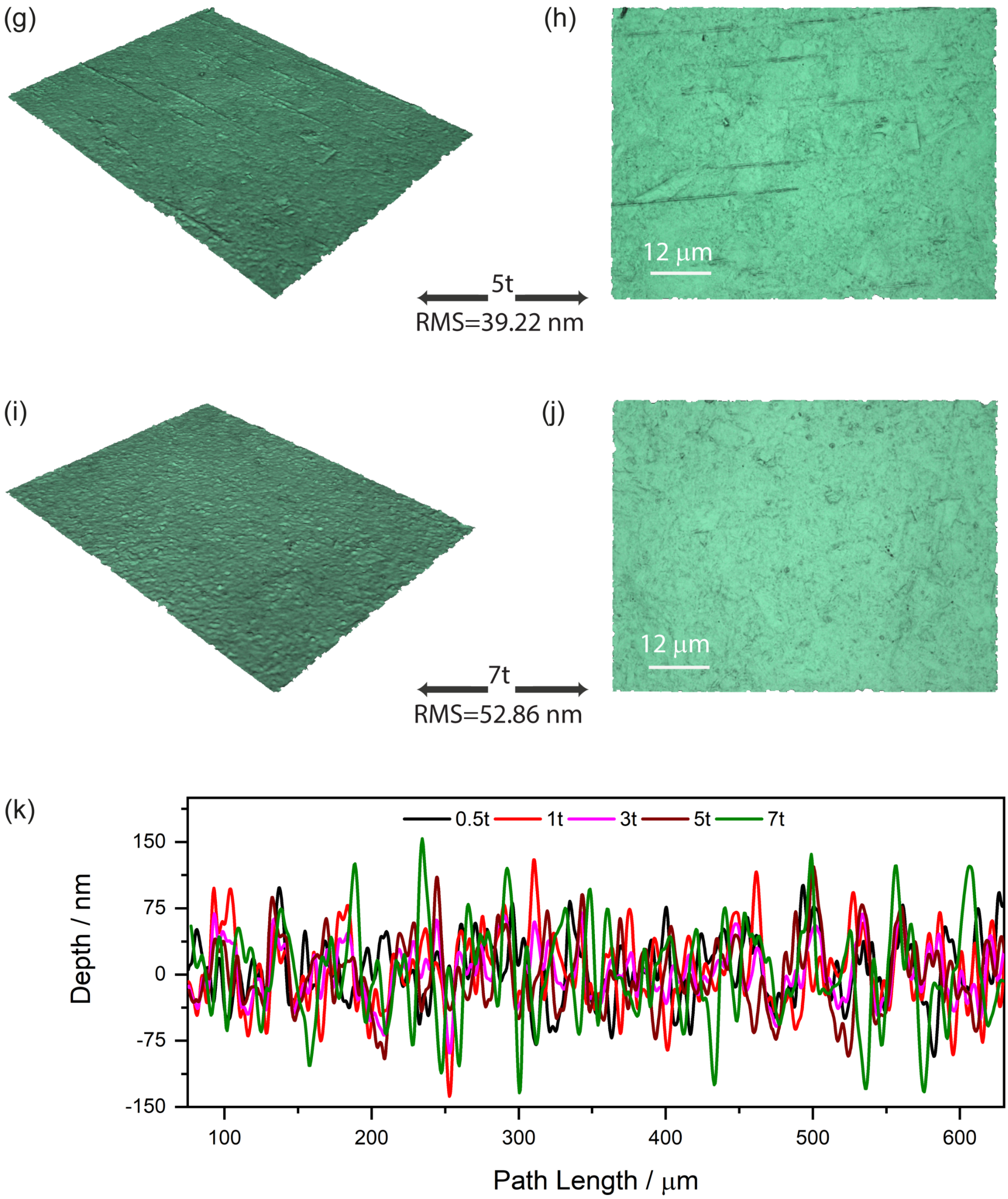

Figure S8: HKUST-1-T pellet surface roughness characterization using Alicona Infinite Focus Microscope at 20× optical magnification: (a)-(b) 0.5 ton, (c)-(d) 1 ton, (e)-(f) 3 ton, (g)-(h) 5 ton, (i)-(j) 7 ton, (k) pellet roughness profile by using the profile line width of 80 μm, respectively. (RMS=Root mean square roughness of profile)

6. Dielectric properties of activated HKUST-1

6.1 Real part of dielectric constant (ε')

6.1.1 HKUST-1-S pellets

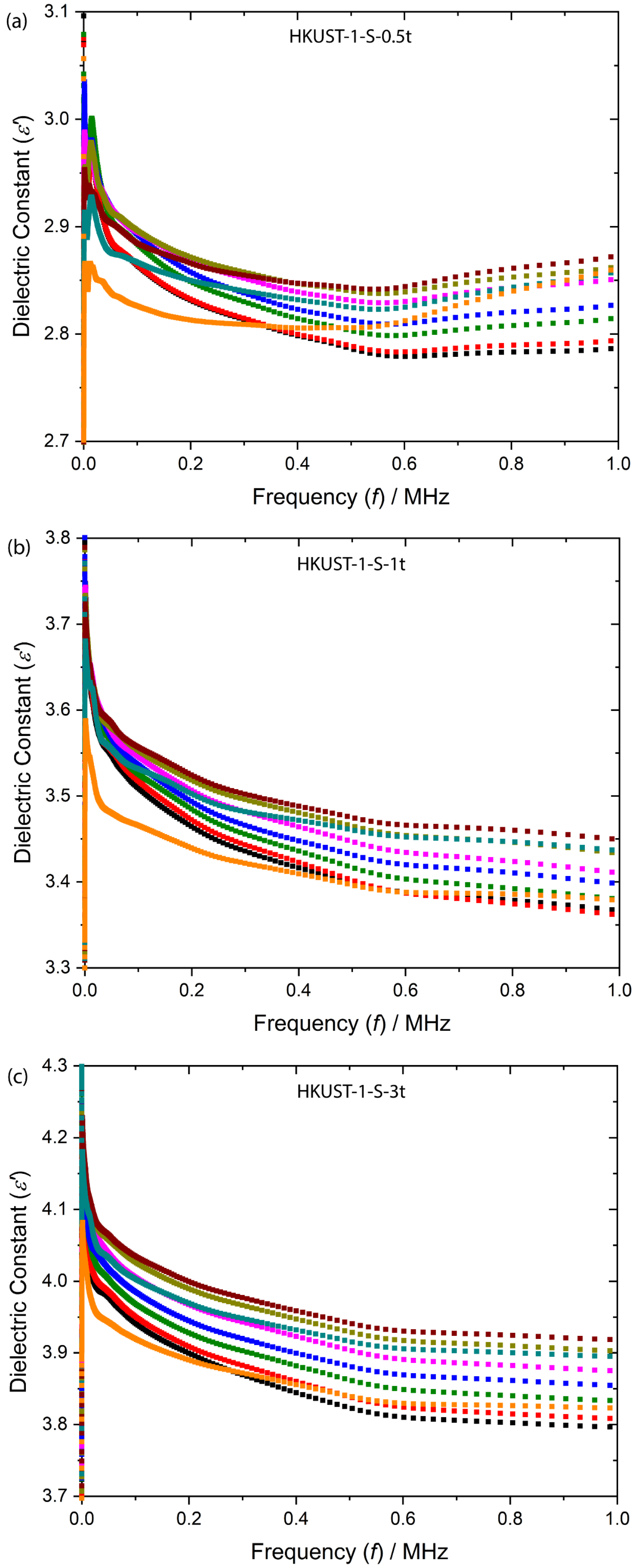

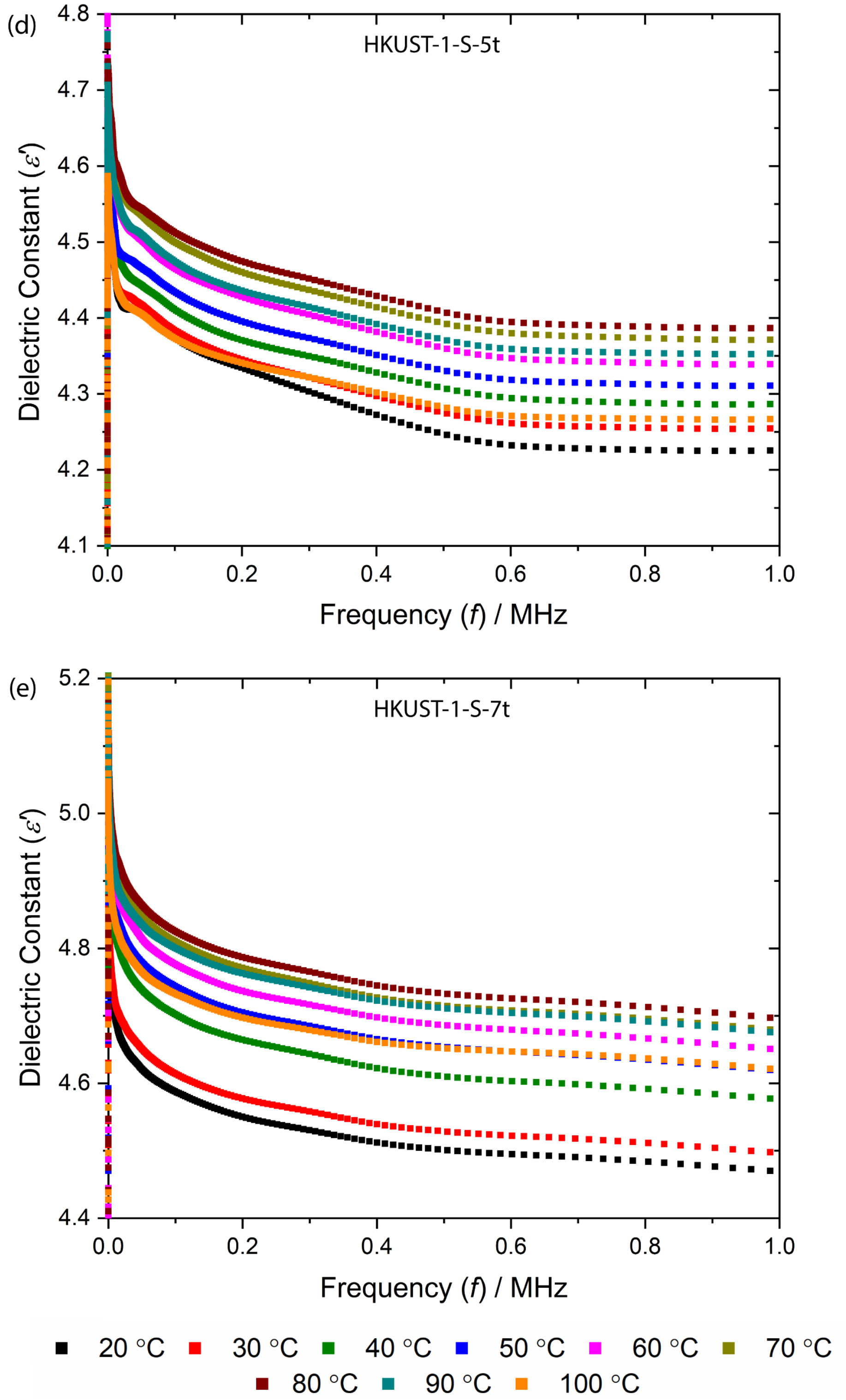

Figure S9: Temperature dependent real part of the dielectric constant as a function of frequency for HKUST-1-S pellets prepared under a compression load of: (a) 0.5 ton, (b) 1 ton, (c) 3 ton, (d) 5 ton and (e) 7 ton, corresponding to the pressure of 36.96, 73.92, 221.76, 369.6 and 517.44 MPa, respectively

6.1.2 HKUST-1-T pellets

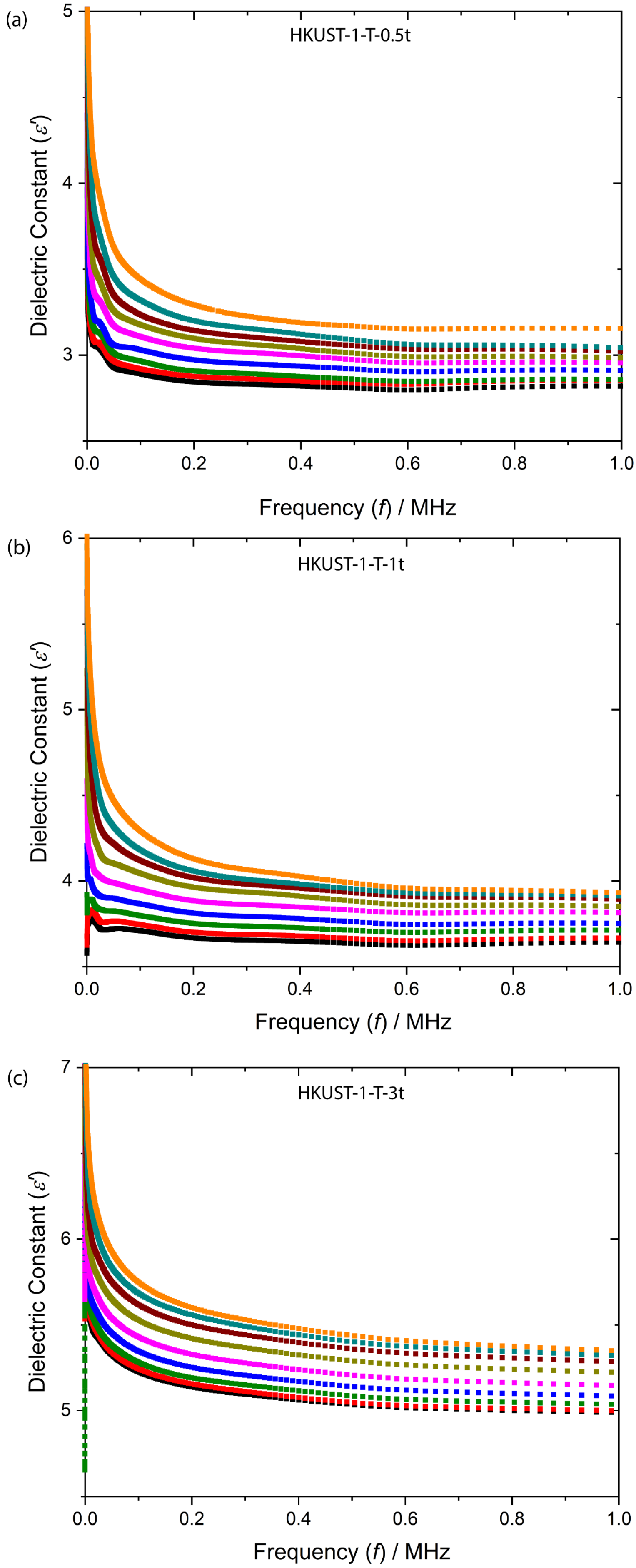

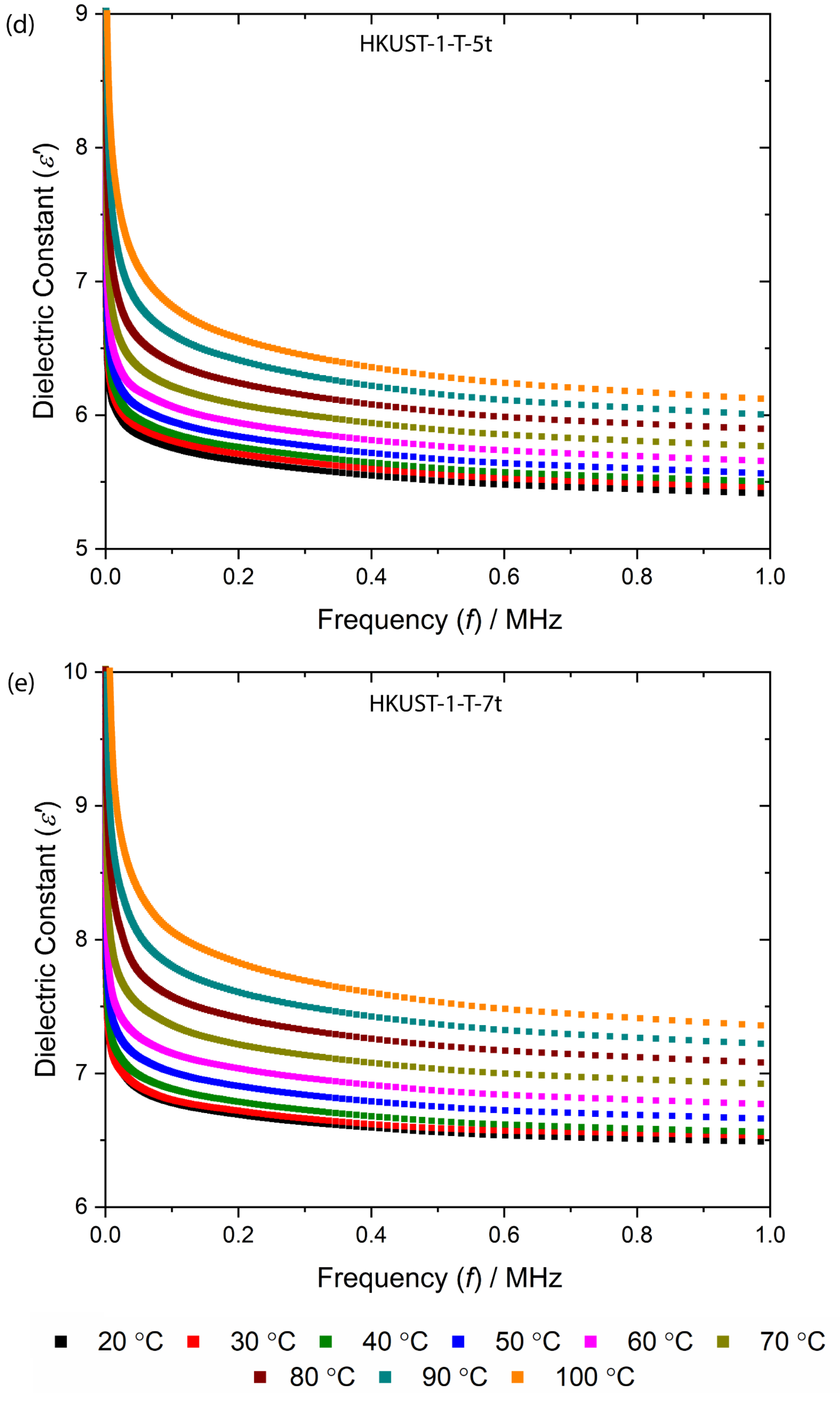

Figure S10: Temperature dependent real part of dielectric constant as a function of frequency for HKUST-1-T pellets: (a) 0.5 ton, (b) 1 ton, (c) 3 ton, (d) 5 ton and (e) 7 ton.

6.2 Imaginary part of dielectric constant (ε'')

6.2.1 HKUST-1-S pellets

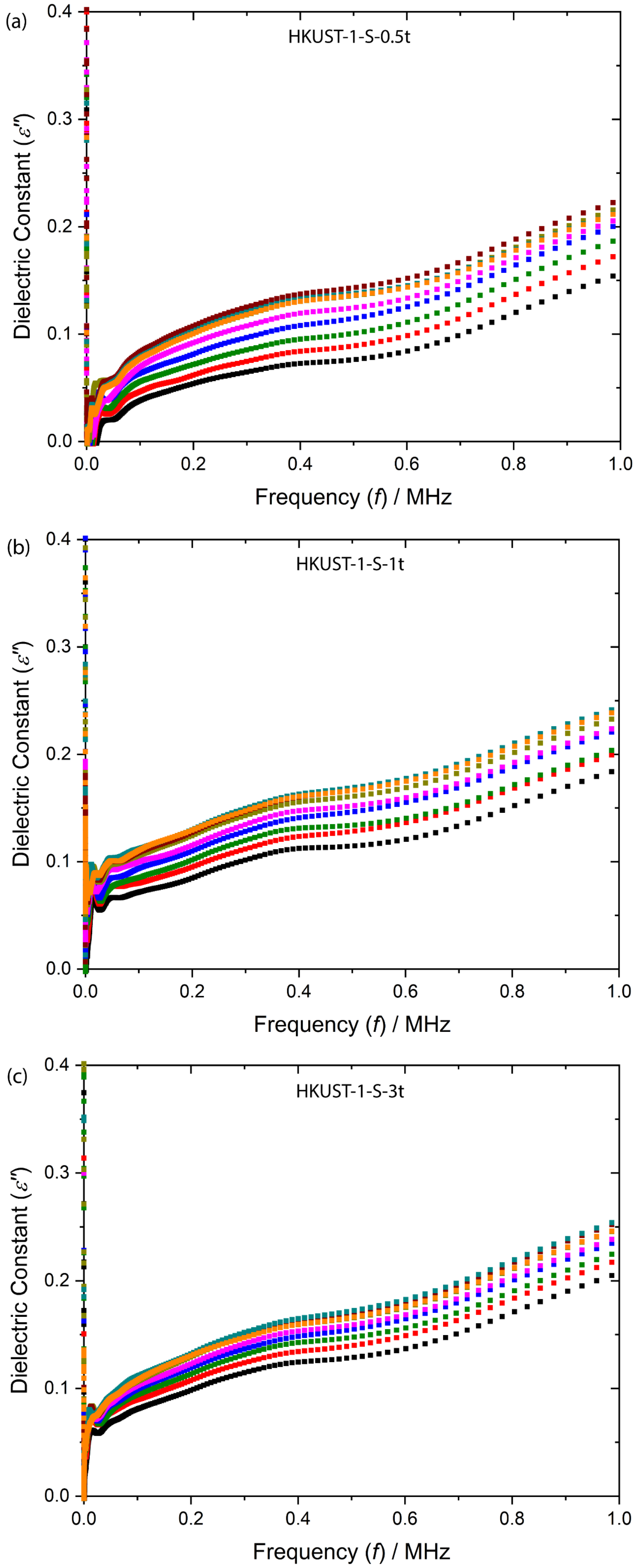

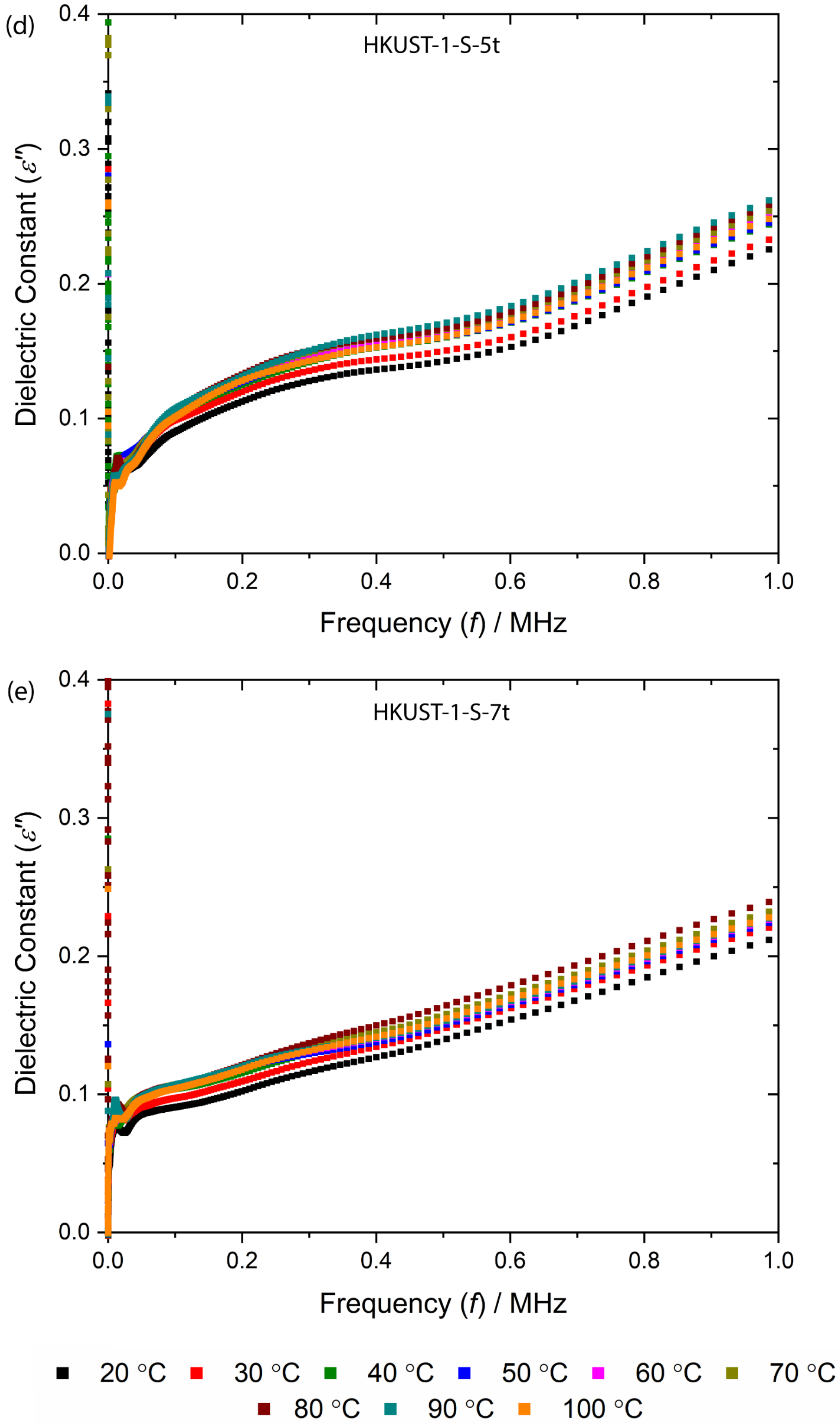

Figure S11: Temperature dependent imaginary part of the dielectric constant as a function of frequency for HKUST-1-S pellets prepared under a compression load of: (a) 0.5 ton, (b) 1 ton, (c) 3 ton, (d) 5 ton and (e) 7 ton, corresponding to the pressure of 36.96, 73.92, 221.76, 369.6 and 517.44 MPa, respectively.

6.2.2 HKUST-1-T pellets

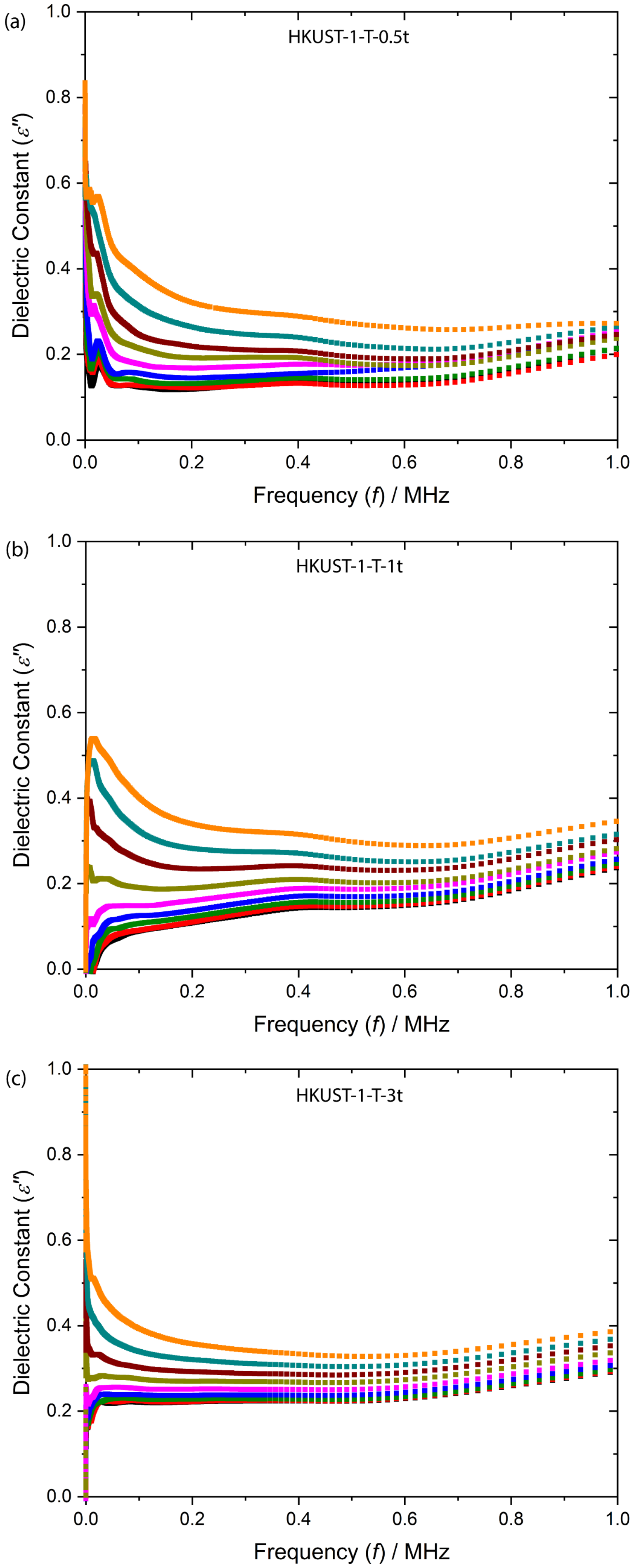

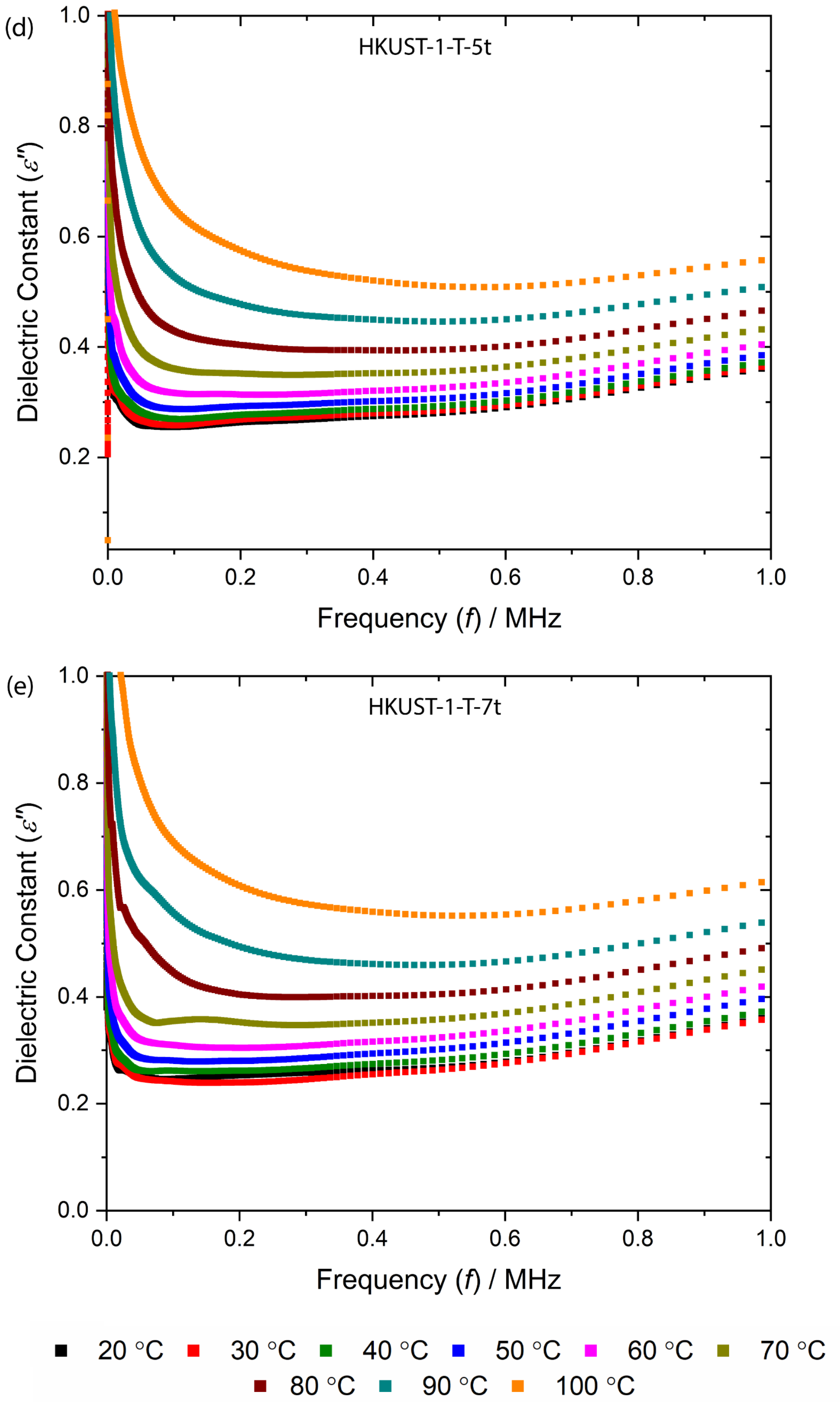

Figure S12: Temperature dependent Imaginary part of dielectric constant as a function of frequency for HKUST-1-T pellets: (a) 0.5 ton, (b) 1 ton, (c) 3 ton, (d) 5 ton and (e) 7 ton.

6.3 Loss tangent (tan δ)

6.3.1 HKUST-1-S pellets

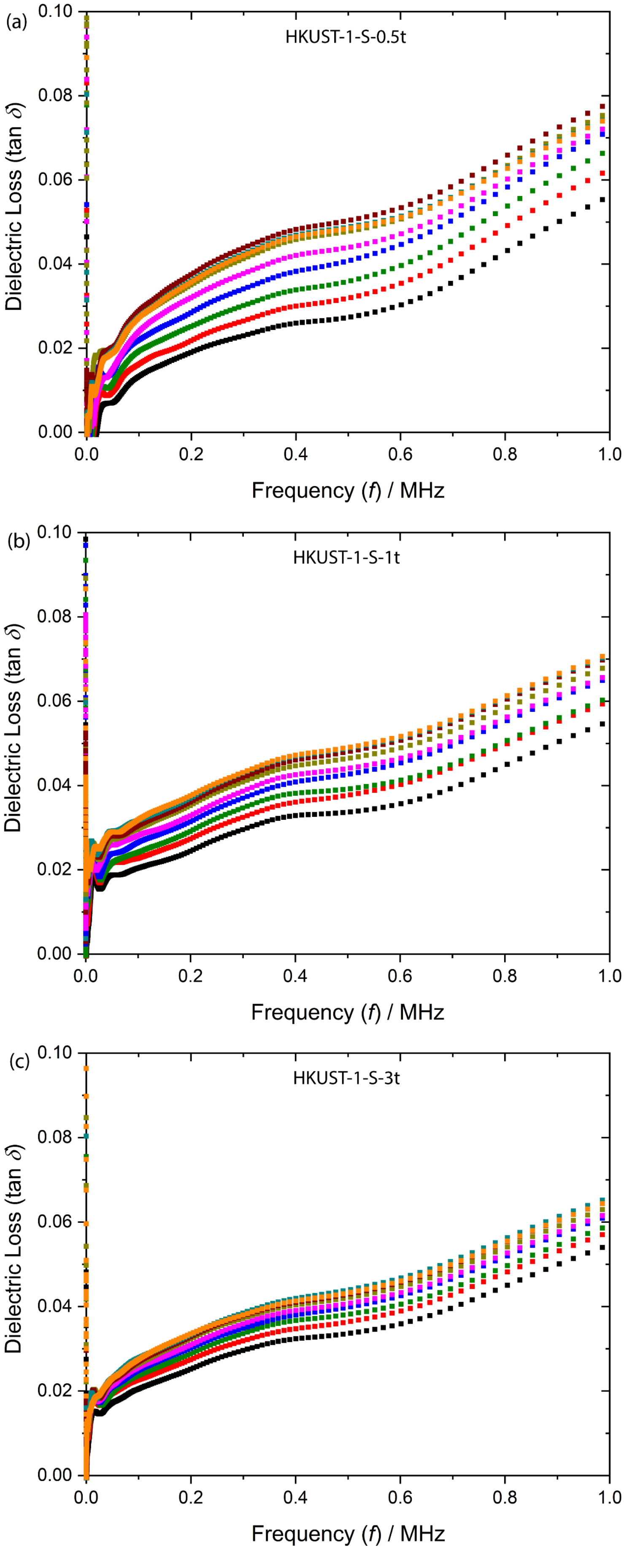

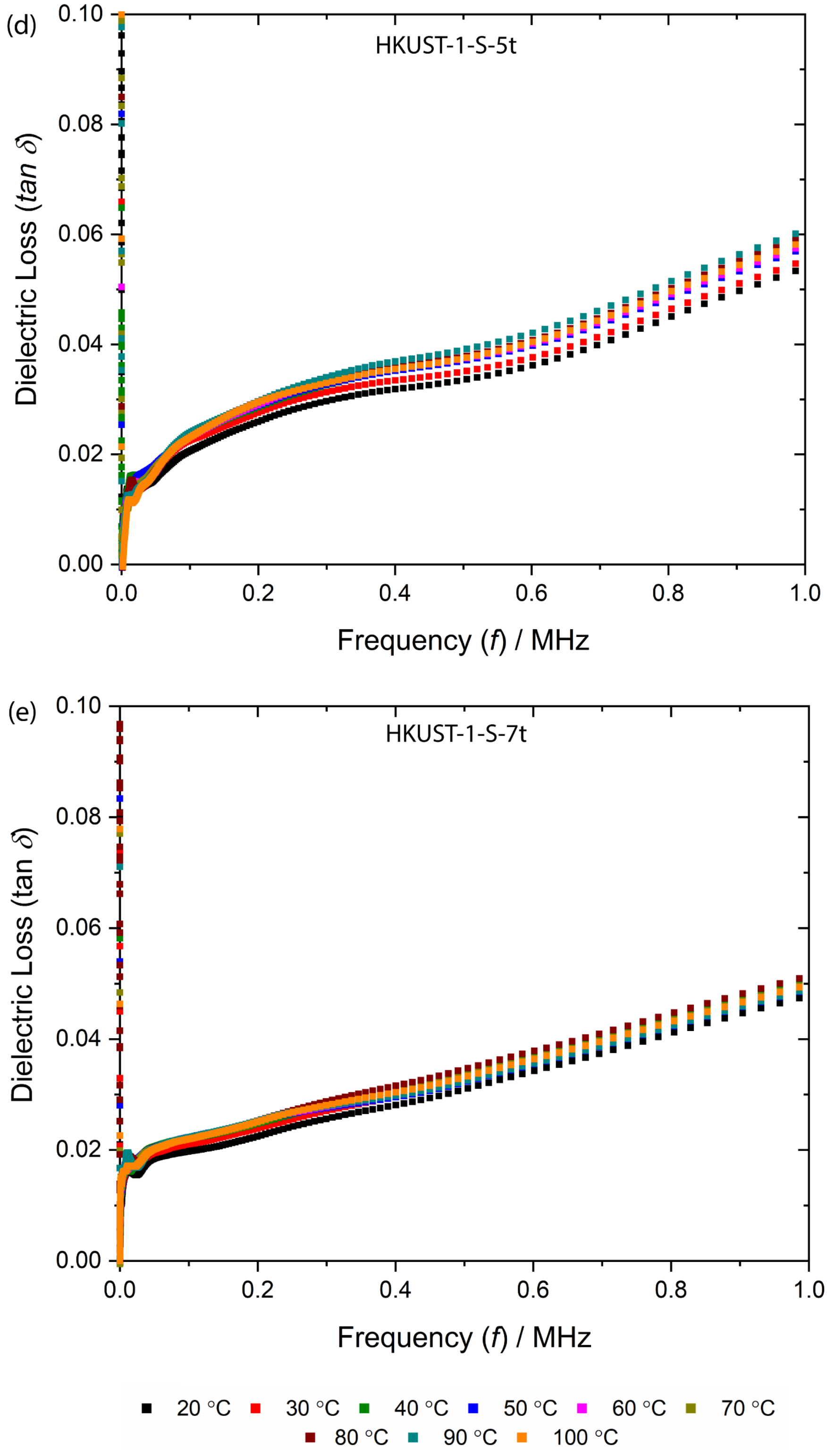

Figure S13: Temperature dependent dielectric loss as a function of frequency for HKUST-1-S pellets prepared under a compression load of: (a) 0.5 ton, (b) 1 ton, (c) 3 ton, (d) 5 ton and (e) 7 ton, corresponding to the pressure of 36.96, 73.92, 221.76, 369.6 and 517.44 MPa, respectively.

6.3.2 HKUST-1-T pellets

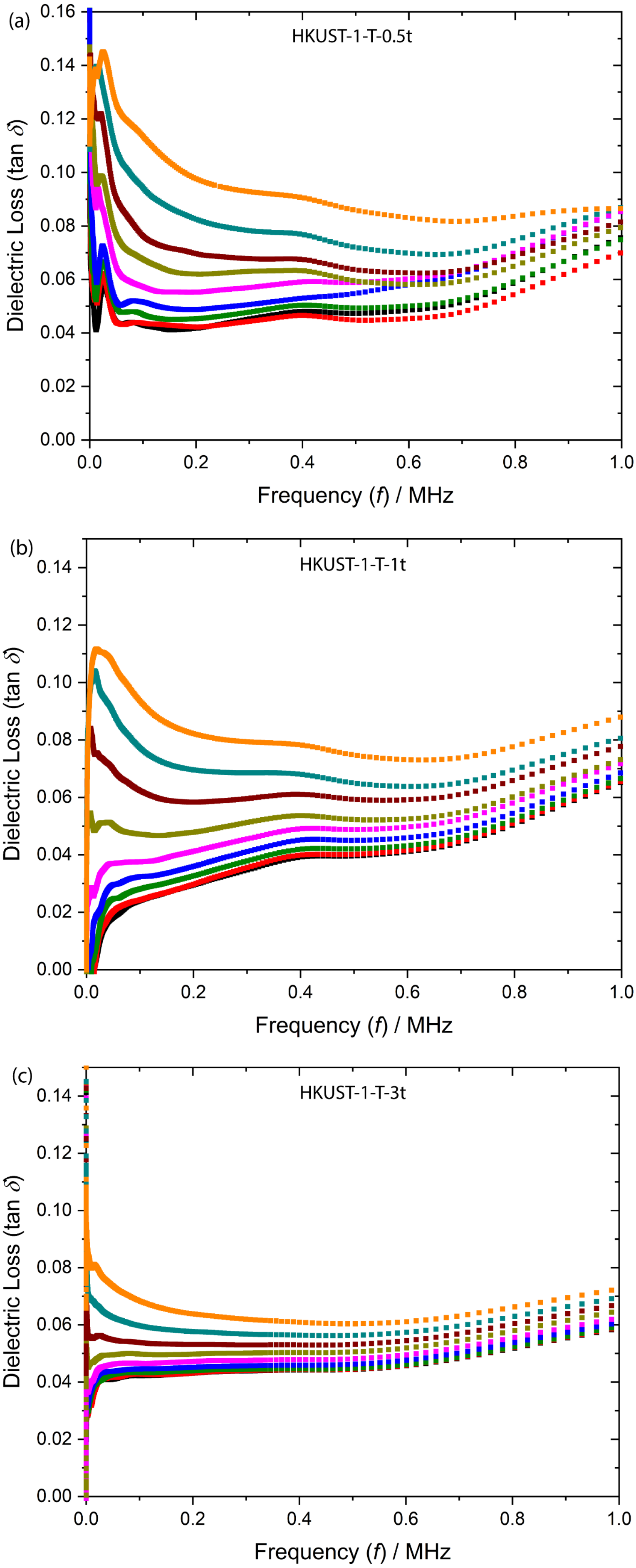

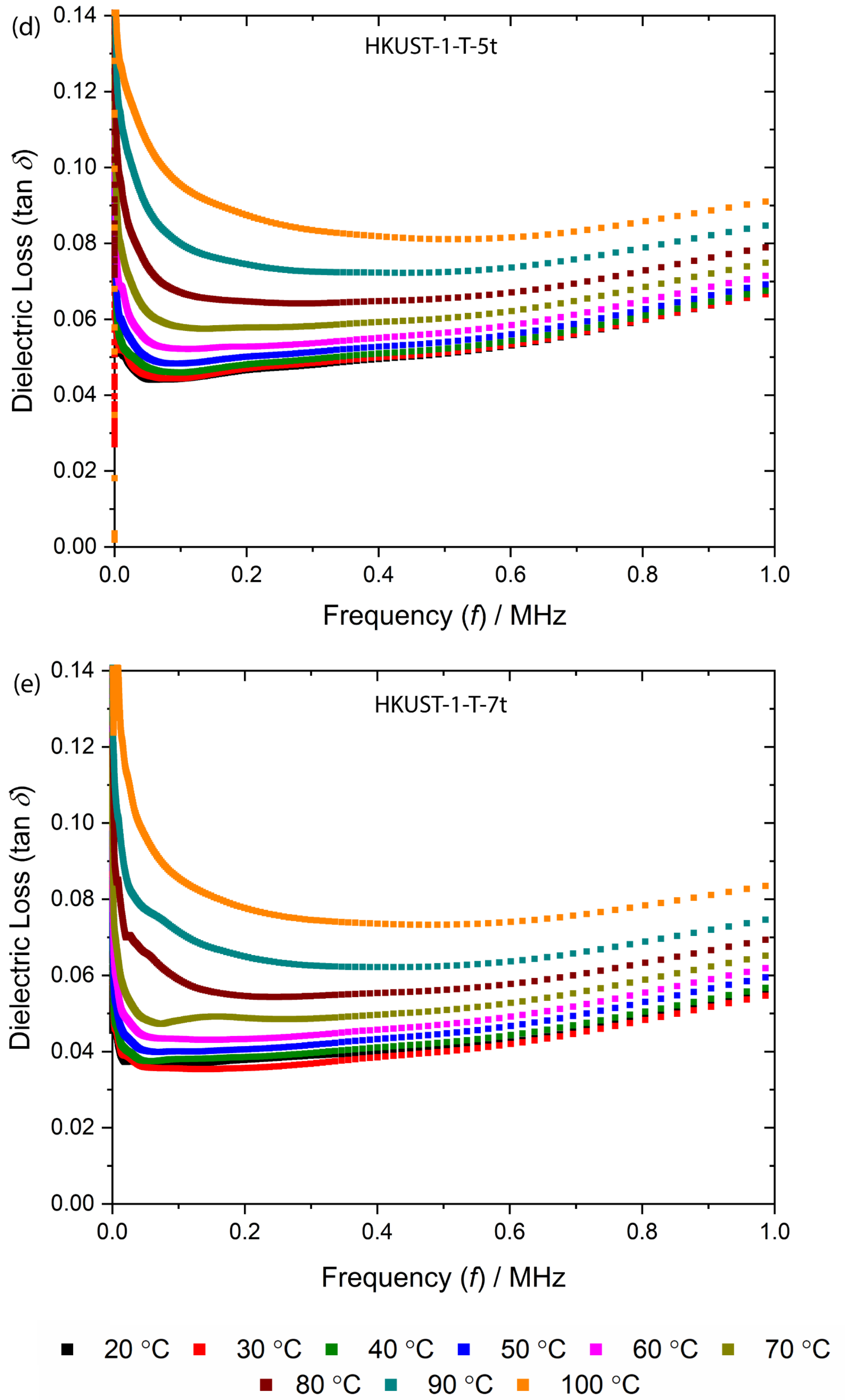

Figure S14: Temperature dependent dielectric loss as a function of frequency for HKUST-1-T pellets: (a) 0.5 ton, (b) 1 ton, (c) 3 ton, (d) 5 ton and (e) 7 ton.

7 Dielectric properties under ambient conditions (44% RH)

7.1 Real part of dielectric constant (ε')

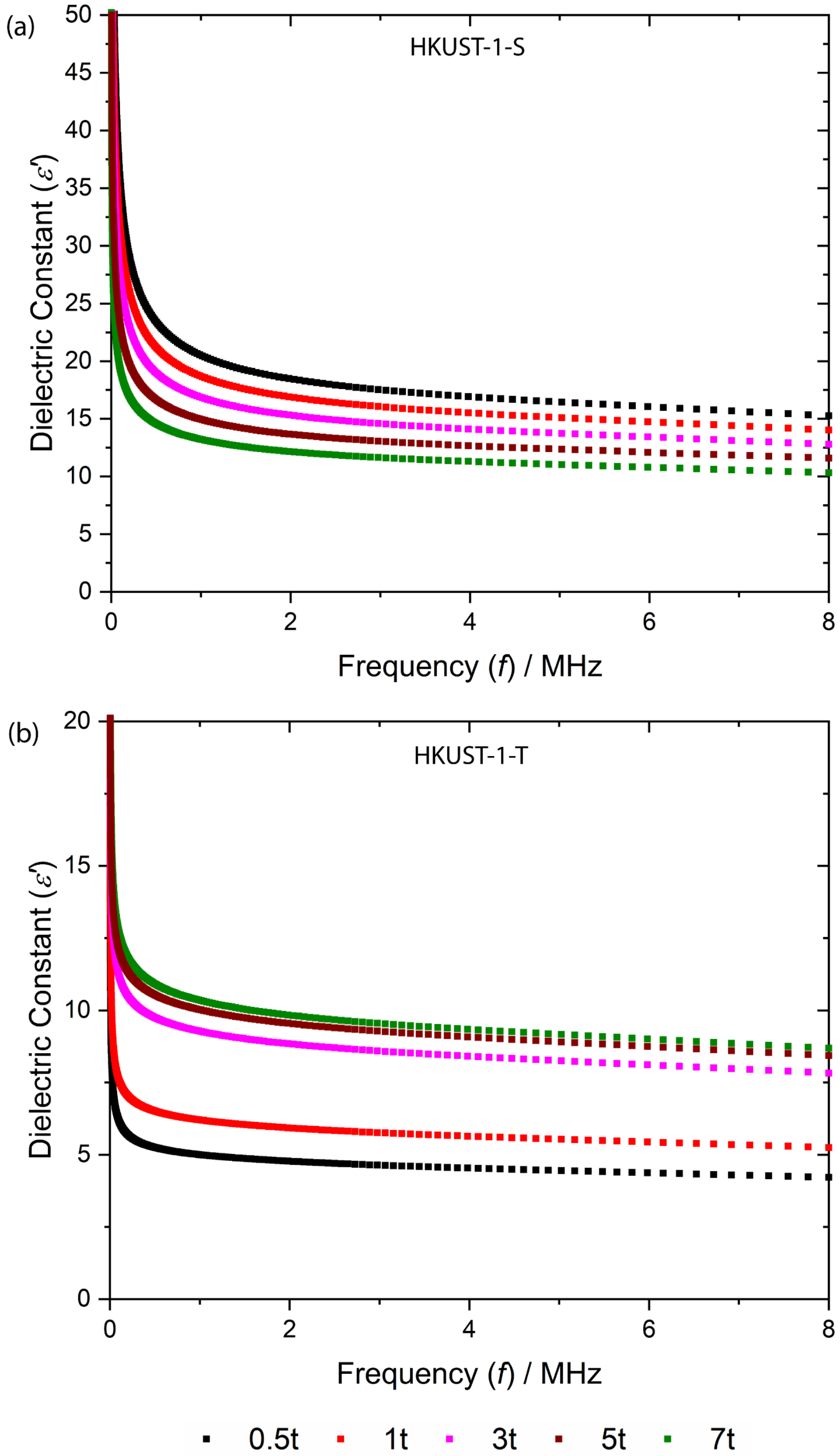

Figure S15: Real part of dielectric constant of (a) HKUST-1-S and (b) HKUST-1-T pellets at ambient condition (44% RH). The HKUST-1-T pellets shows relatively lower ε' value over HKUST-1-S pellets due to the presence of NEt_3 molecule in the pore causing lesser moisture adsorption. In the case of HKUST-1-T samples, the ε' value increases with pelleting pressure up to a certain extent due to the increase in the structural density and interaction between the water and guest molecule, whereas the decrease in the HKUST-1-S samples is mainly contributed by the water expulsion causing reduction in the overall dipole moment..

7.2 Imaginary part of dielectric constant (ε'')

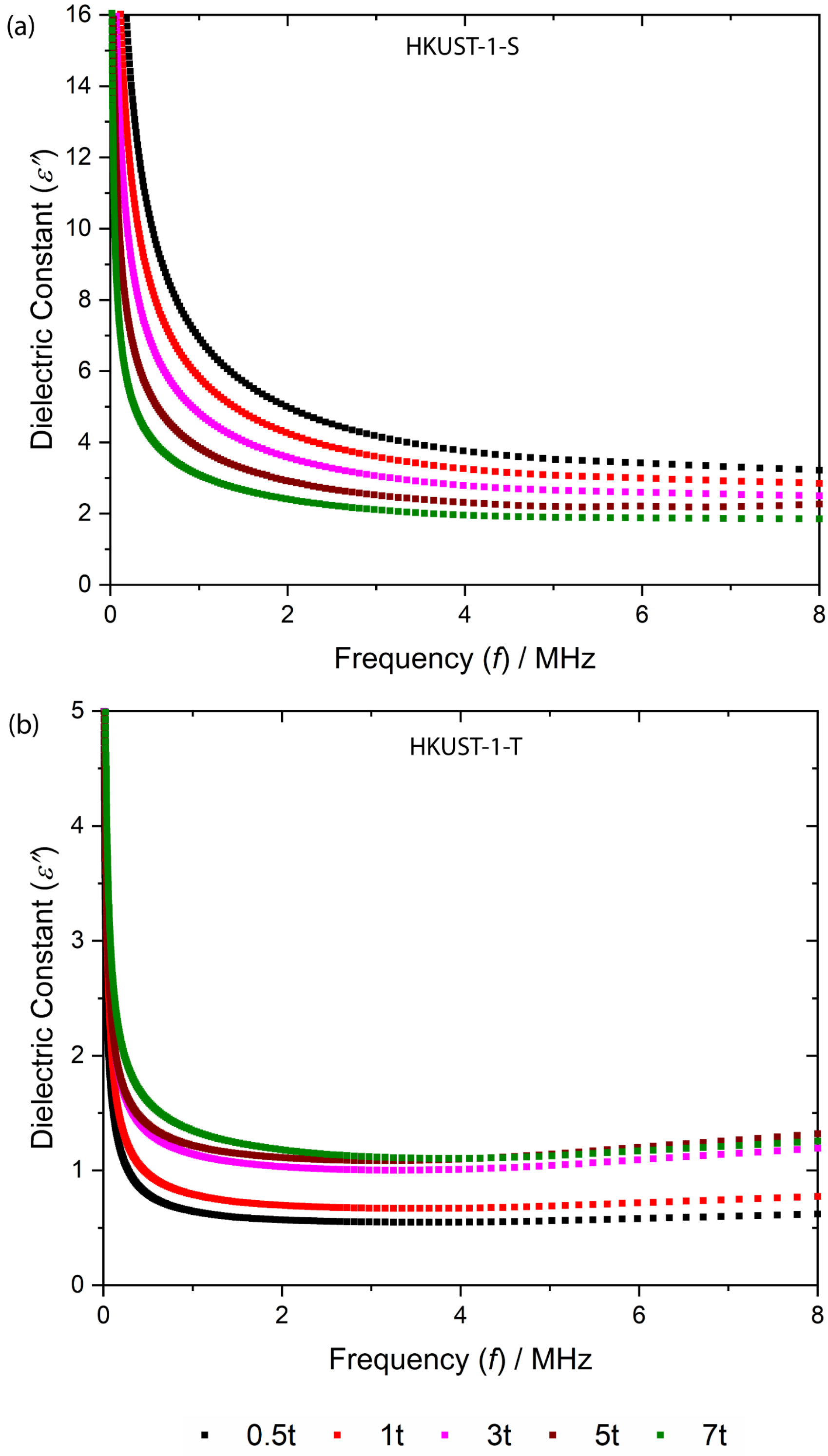

Figure S16: Imaginary part of dielectric constant of (a) HKUST-1-S and (b) HKUST-1-T pellets at ambient condition.

7.3 Loss Tangent (tan δ)

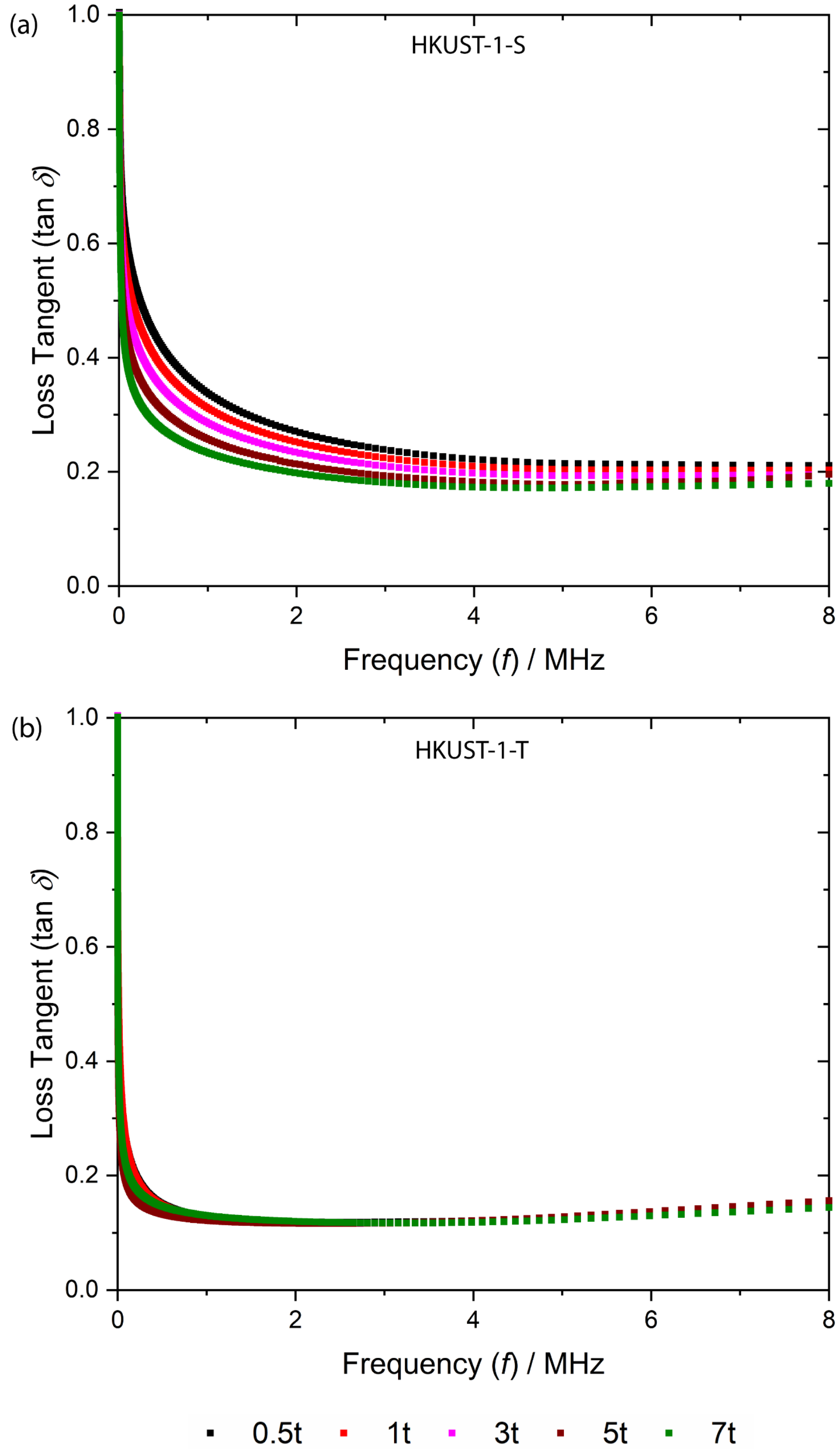

Figure S17: Dielectric loss of (a) HKUST-1-S and (b) HKUST-1-T pellets at ambient condition.

8 Conductivity measurements

8.1 AC conductivity (σ_{AC})

8.1.1 HKUST-1-S pellets

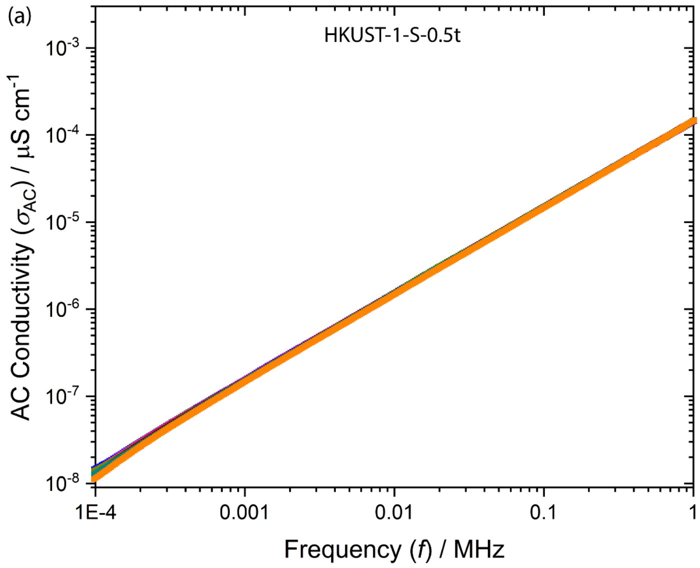

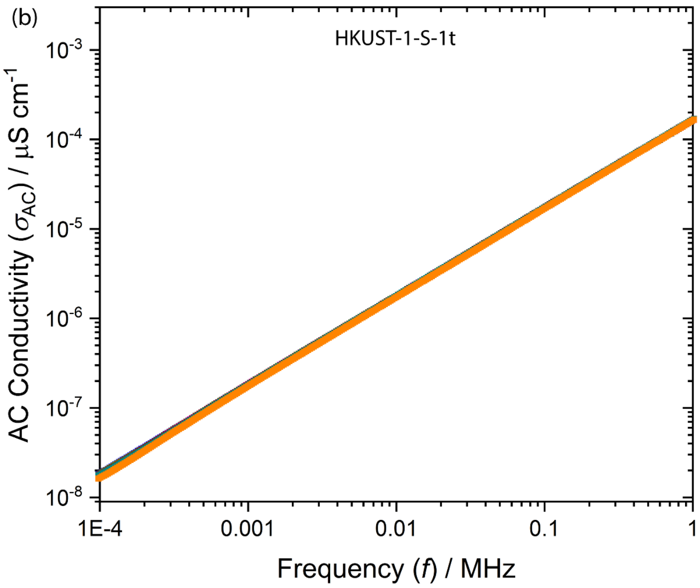

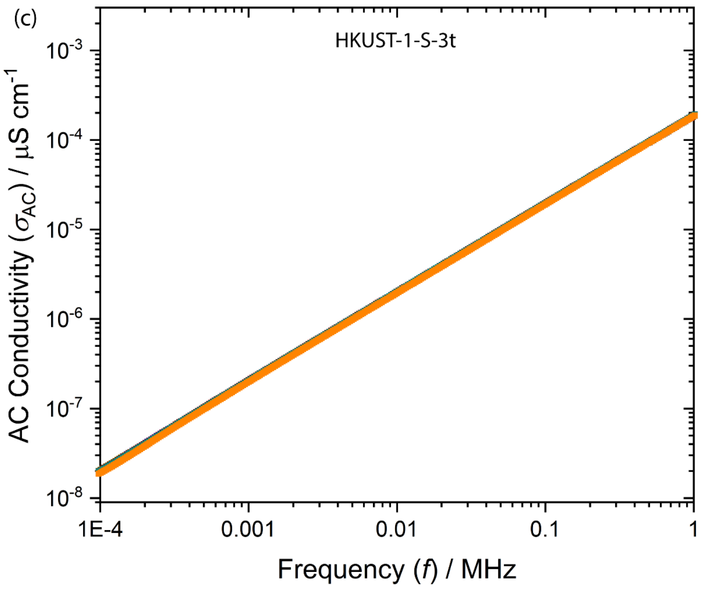

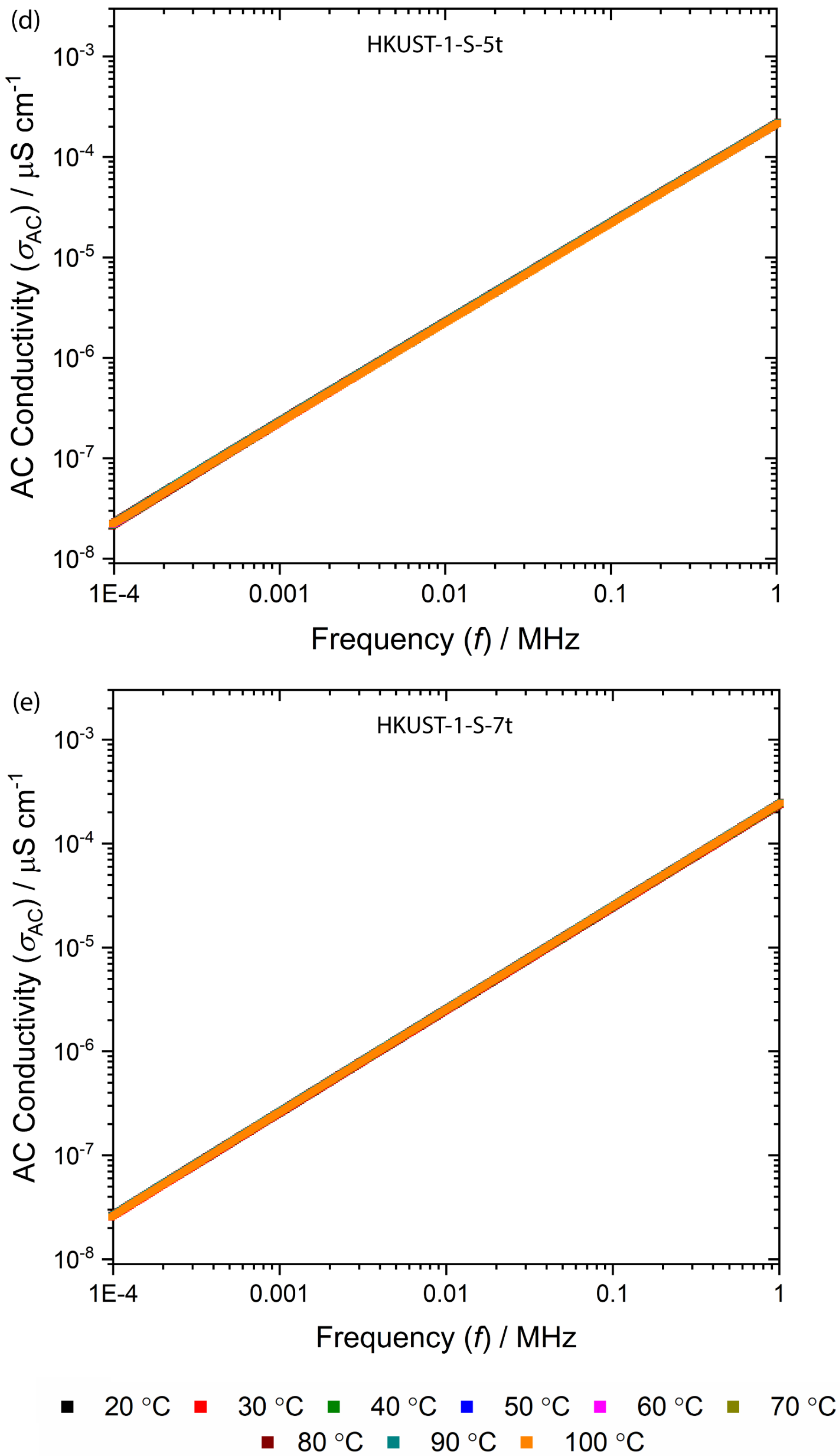

Figure S18: Temperature dependent Ac conductivity as a function of frequency for HKUST-1-S pellets prepared under a compression load of: (a) 0.5 ton, (b) 1 ton, (c) 3 ton, (d) 5 ton and (e) 7 ton, corresponding to the pressure of 36.96, 73.92, 221.76, 369.6 and 517.44 MPa, respectively.

8.1.2 HKUST-1-T pellets

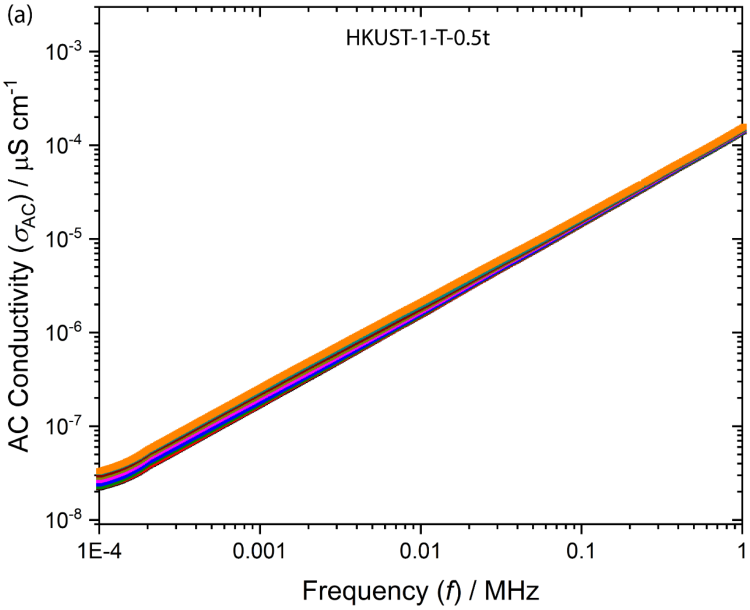

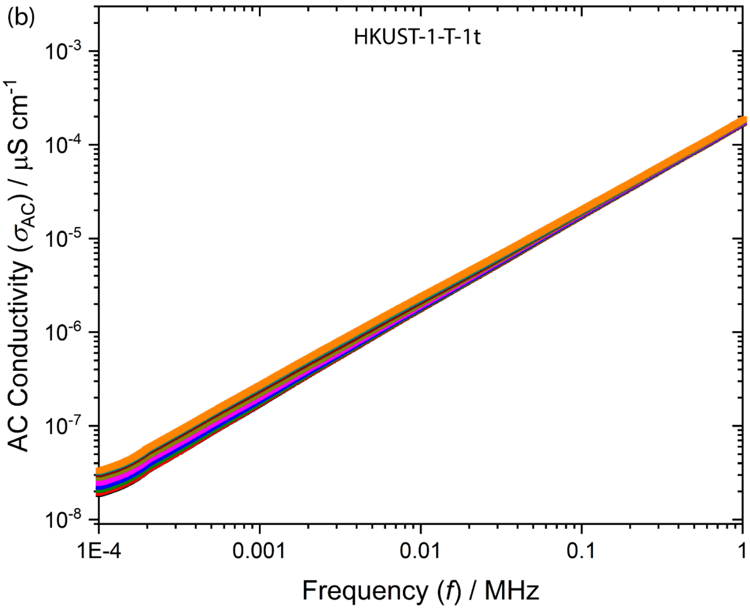

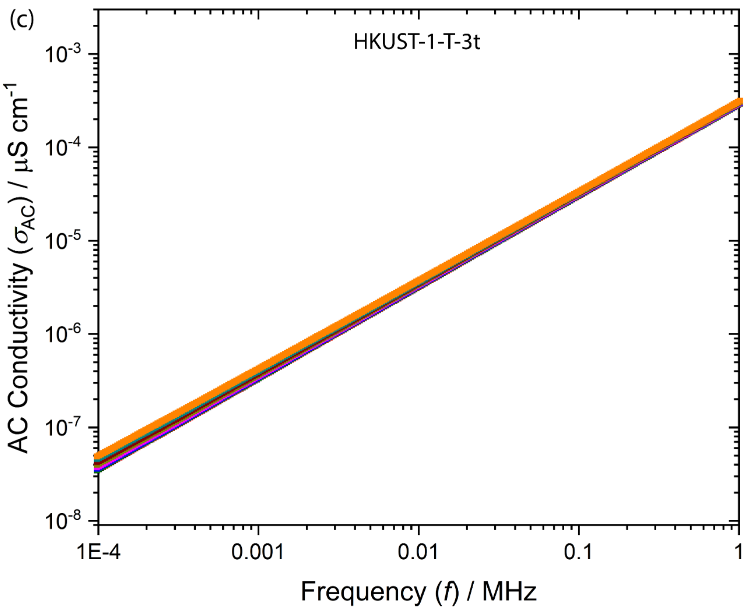

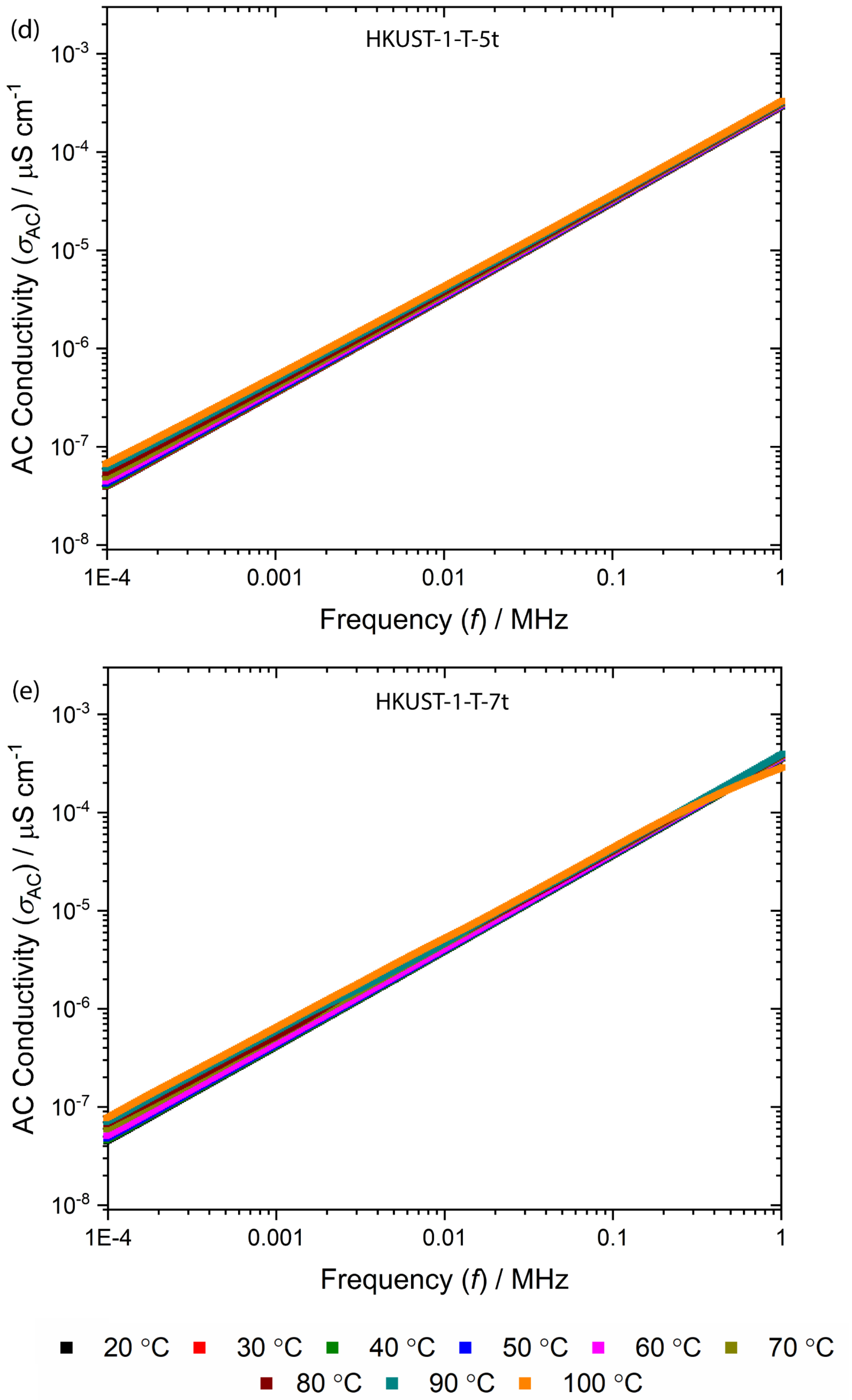

Figure S19: Temperature dependent AC conductivity as a function of frequency for HKUST-1-T pellets: (a) 0.5 ton, (b) 1 ton, (c) 3 ton, (d) 5 ton and (e) 7 ton.

8.2 Impedance measurements (Z^*)

8.2.1 HKUST-1-S pellets

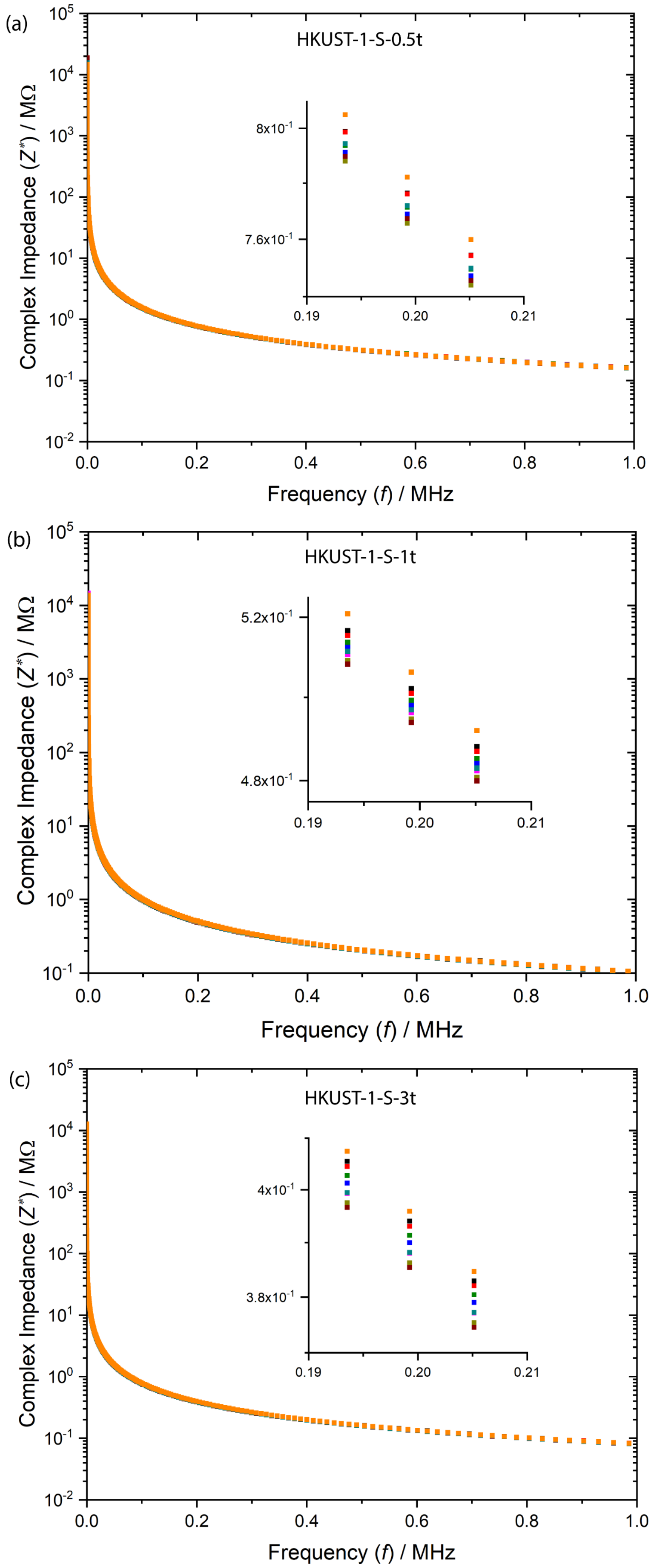

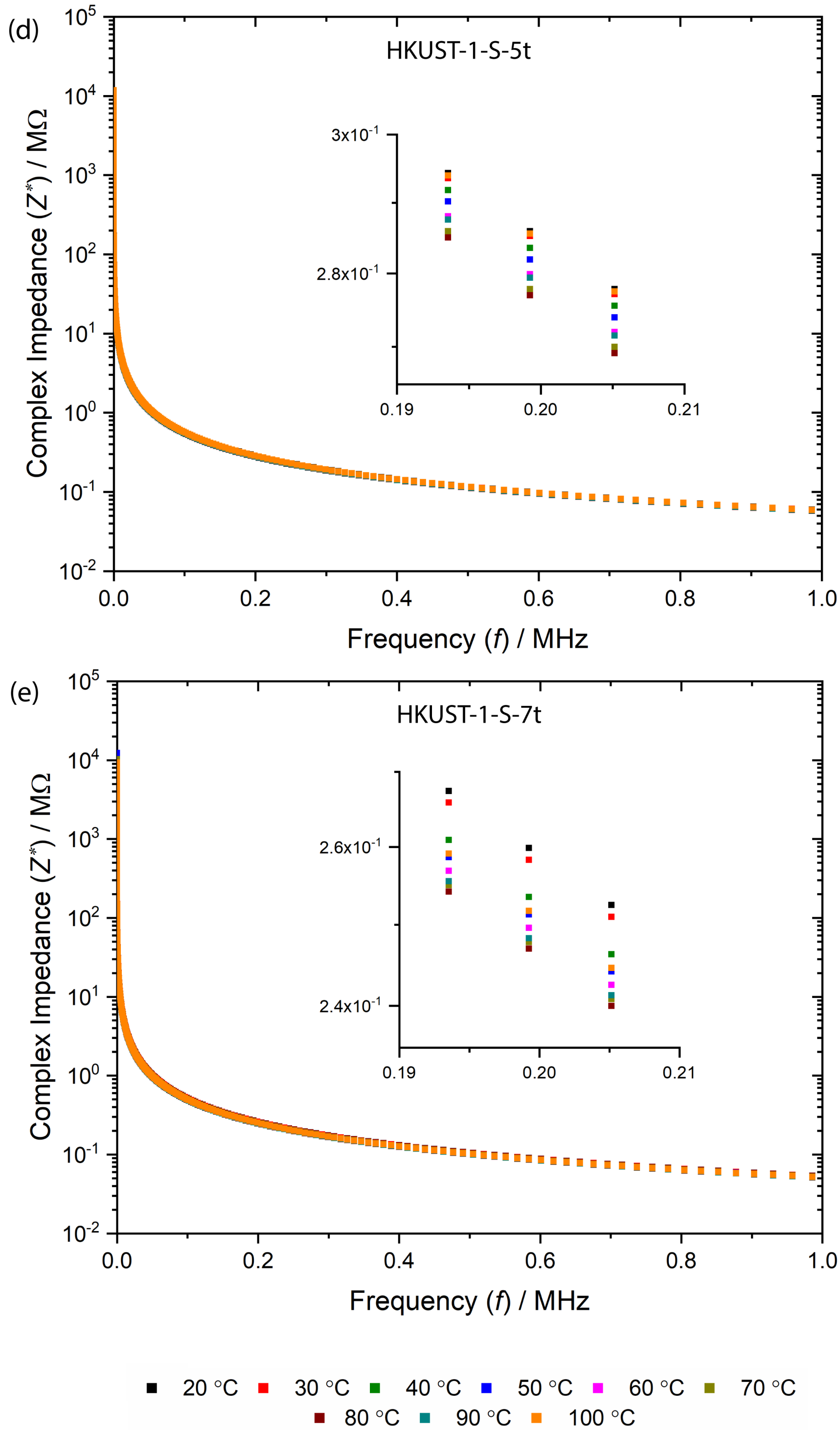

Figure S21: Temperature dependent impedance as a function of frequency for HKUST-1-S pellets prepared under a compression load of: (a) 0.5 ton, (b) 1 ton, (c) 3 ton, (d) 5 ton and (e) 7 ton, corresponding to the pressure of 36.96, 73.92, 221.76, 369.6 and 517.44 MPa, respectively.

8.2.2 HKUST-1-T pellets

(a)

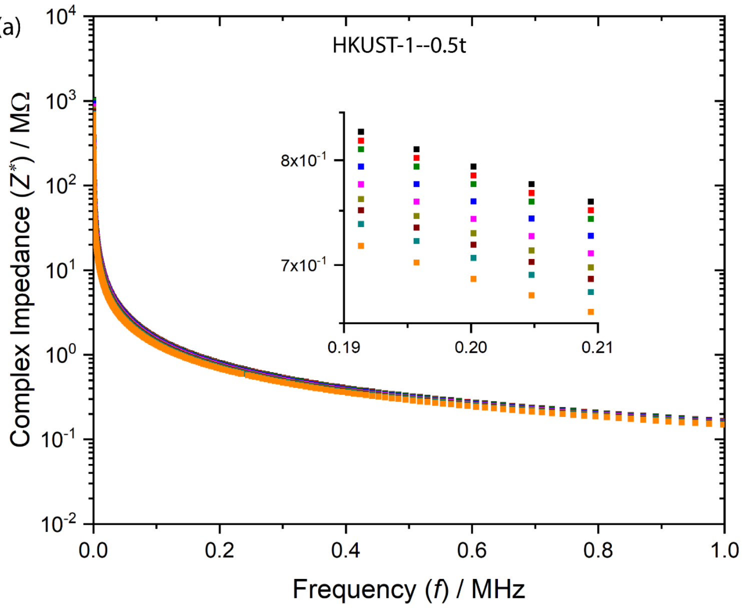

(b)

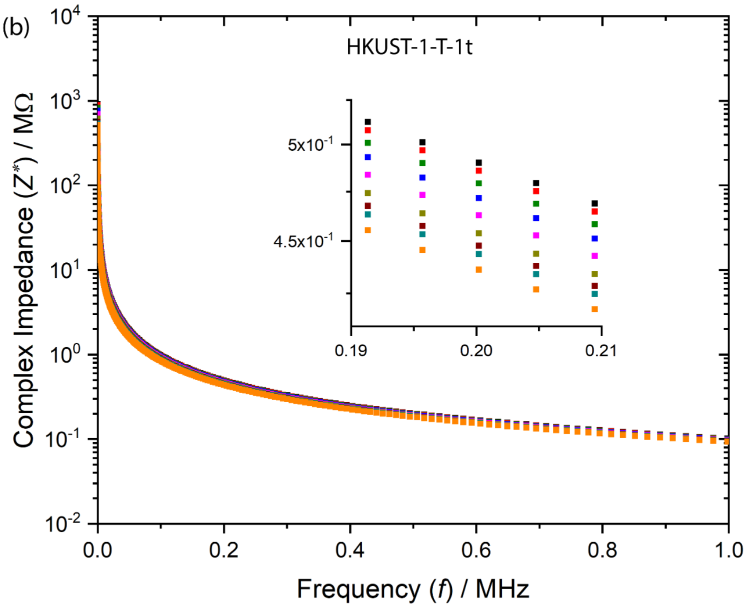

(c)

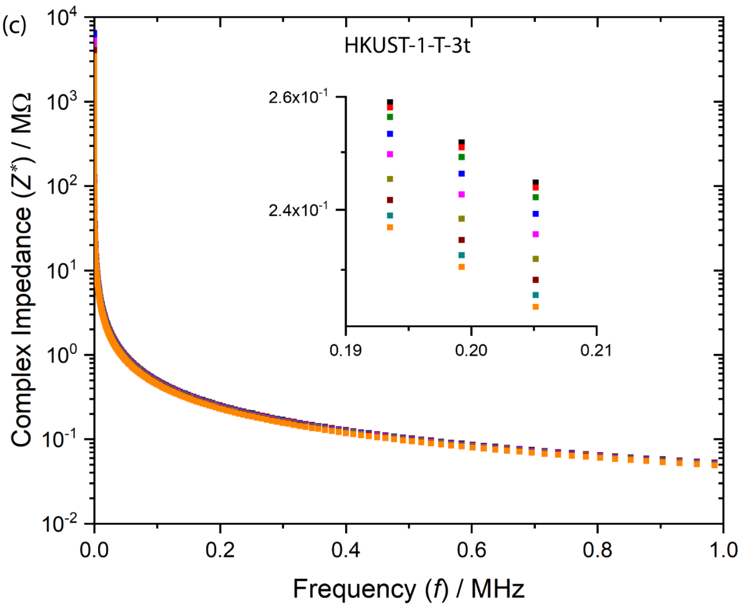

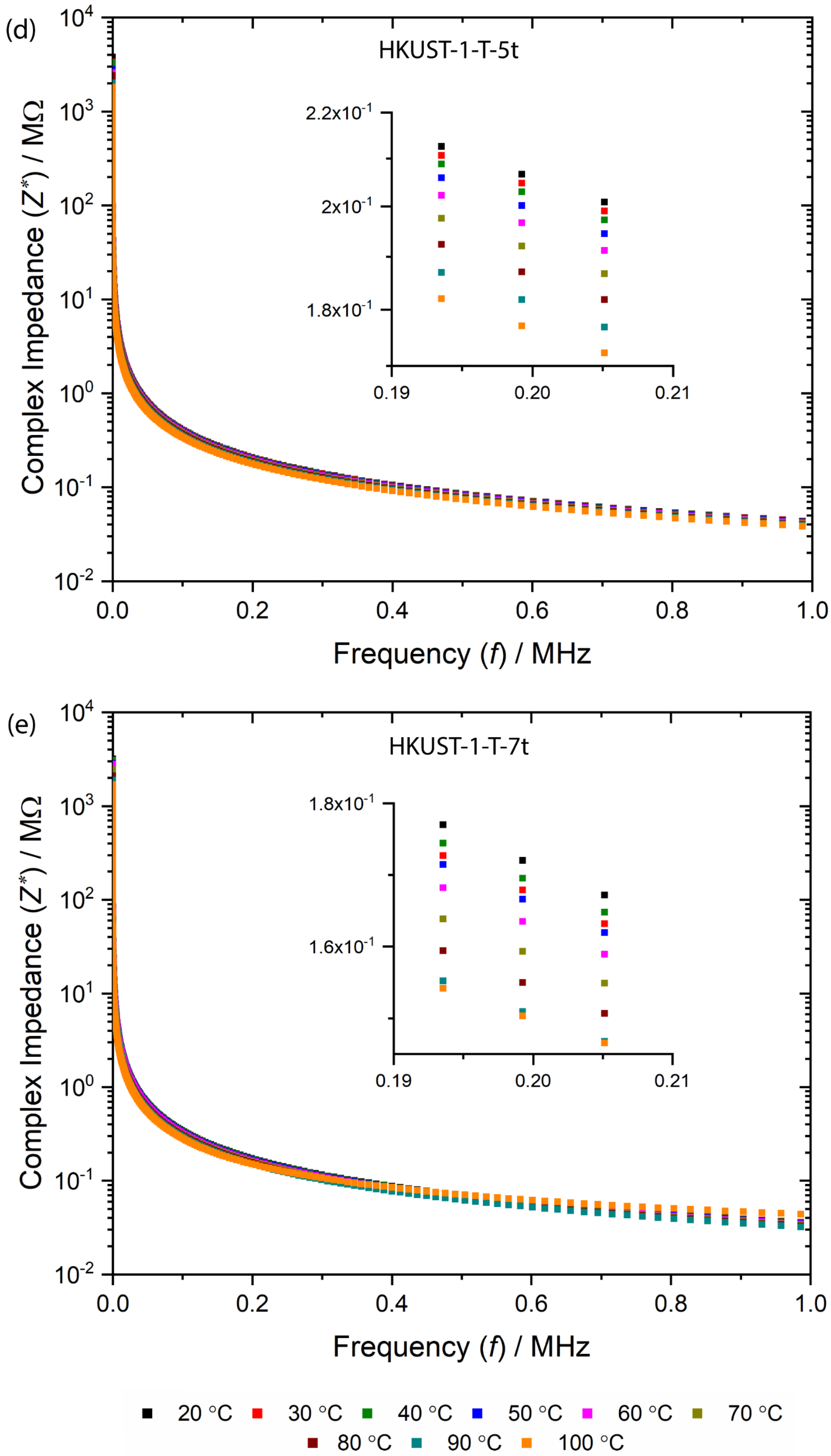

Figure S22: Temperature dependent impedance as a function of frequency for HKUST-1-T pellets: (a) 0.5 ton, (b) 1 ton, (c) 3 ton, (d) 5 ton and (e) 7 ton.

8.2.3 Complex impedance of pellets at ambient conditions (44% RH)

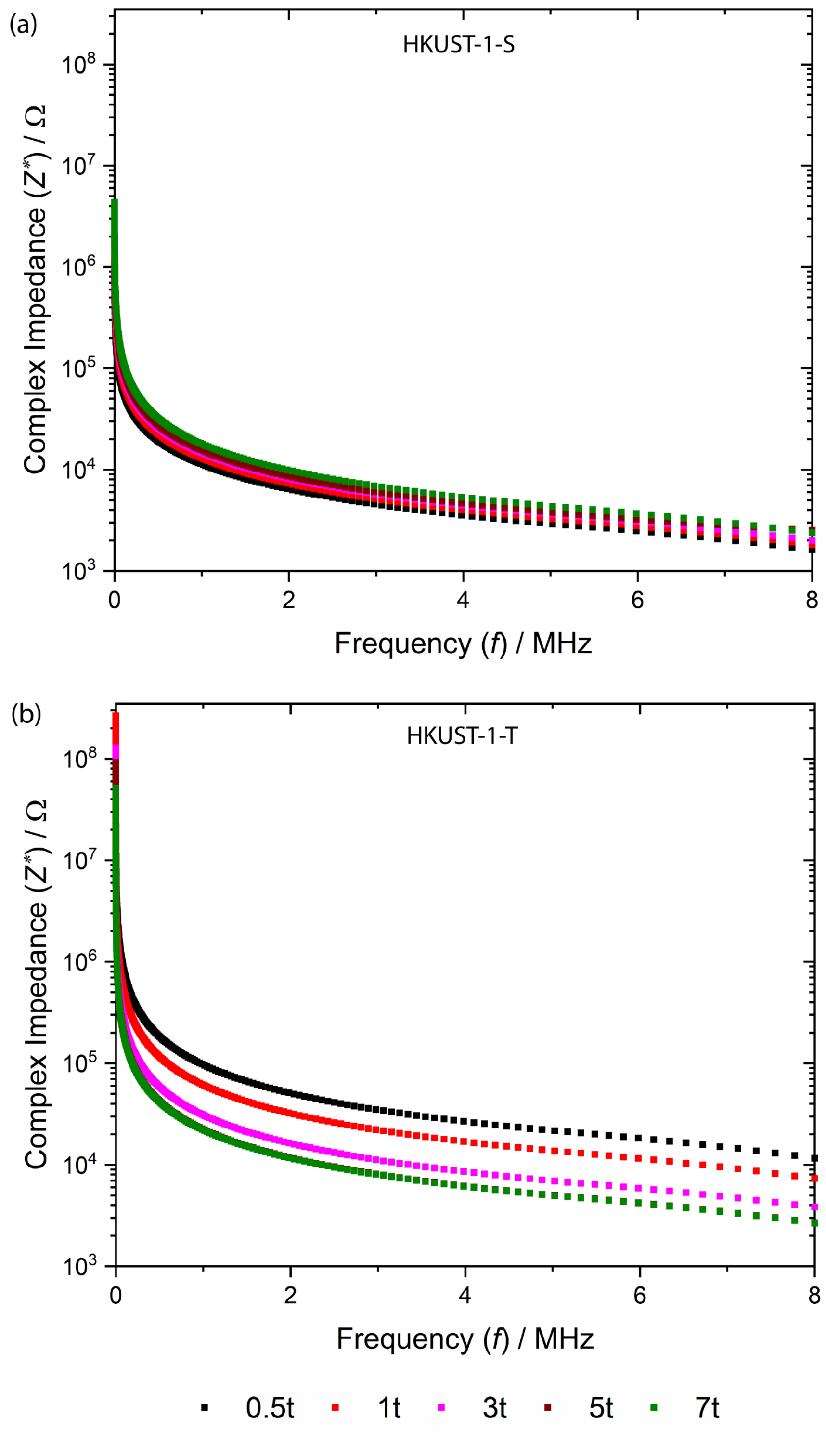

Figure 23: Plot Complex impedance with frequency for (a) HKUST-1-S and (b) HKUST-1-T at ambient condition.

9 Equivalent circuit data fitting of impedance plot

9.1 HKUST-1-S pellets

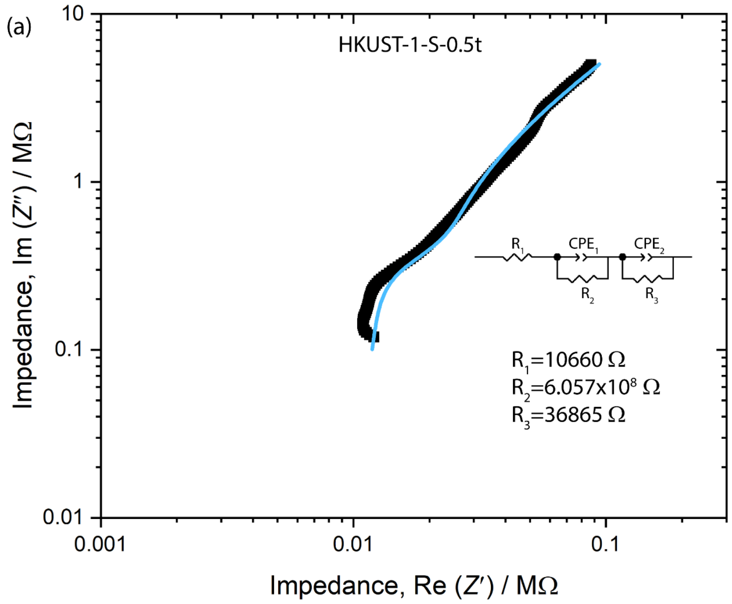

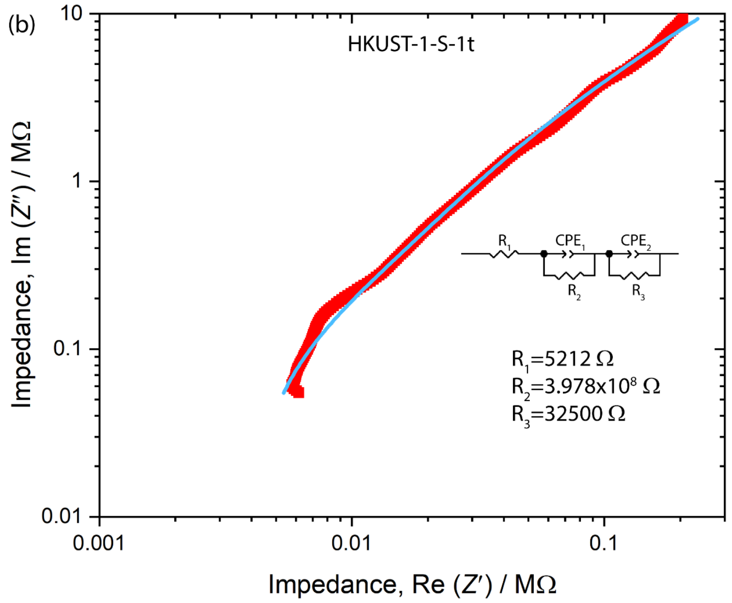

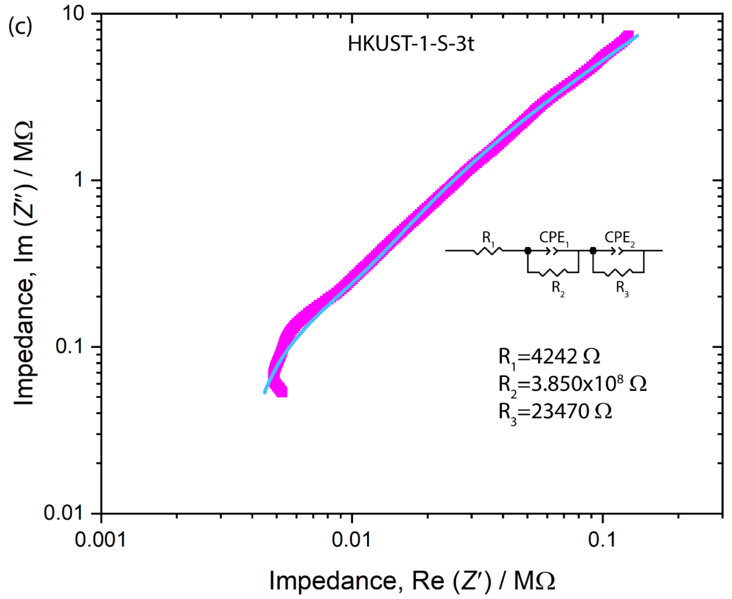

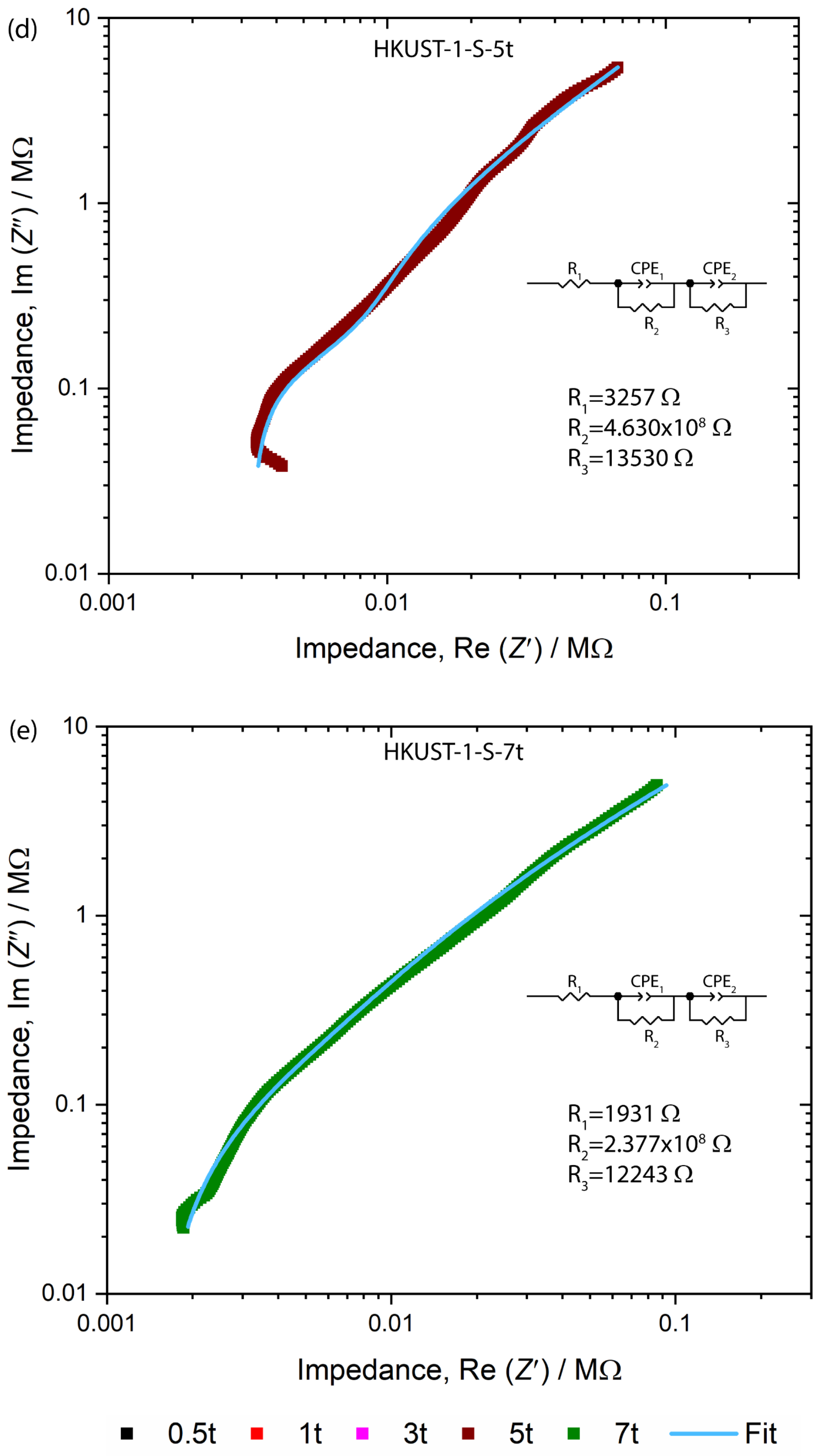

Figure 24: Impedance plot of real impedance vs imaginary impedance with the equivalent circuit curve fit at 20 °C for HKUST-1-S: (a) 0.5 ton, (b) 1 ton, (c) 3 ton, (d) 5 ton and (e) 7 ton, corresponding to the pressure of 36.96, 73.92, 221.76, 369.6 and 517.44 MPa, respectively.

9.2 HKUST-1-T

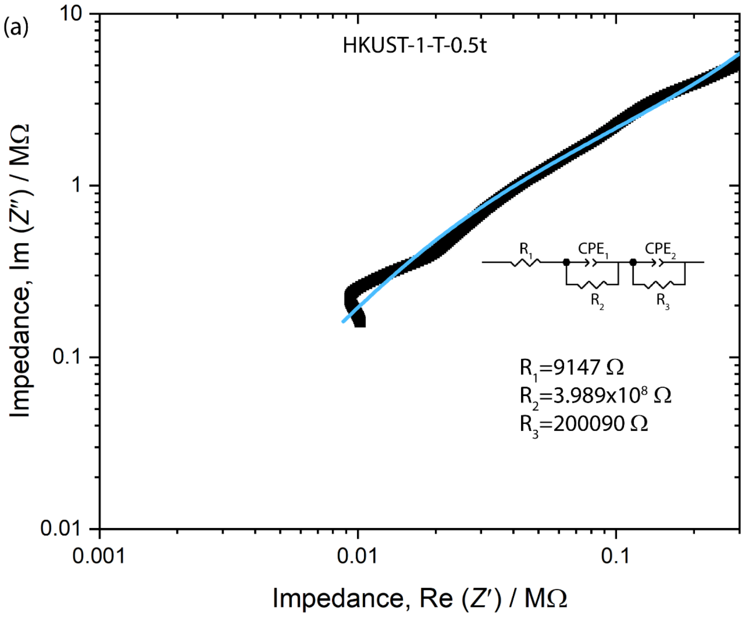

(a)
HKUST-1-T-0.5t
R1=9147 Ω
R2=3.989x10^8 Ω
R3=200090 Ω
Impedance, Im (Z″) / MΩ
Impedance, Re (Z′) / MΩ

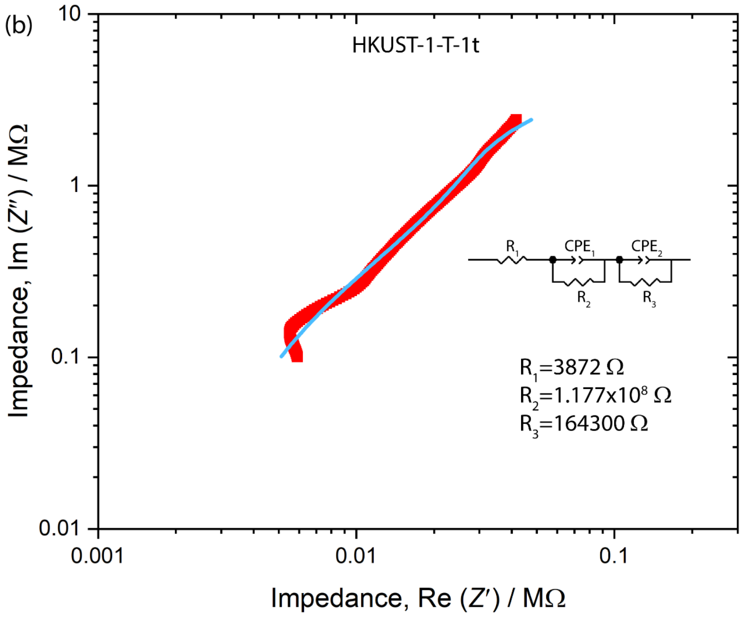

(b)
HKUST-1-T-1t
R1=3872 Ω
R2=1.177x10^8 Ω
R3=164300 Ω
Impedance, Im (Z″) / MΩ
Impedance, Re (Z′) / MΩ

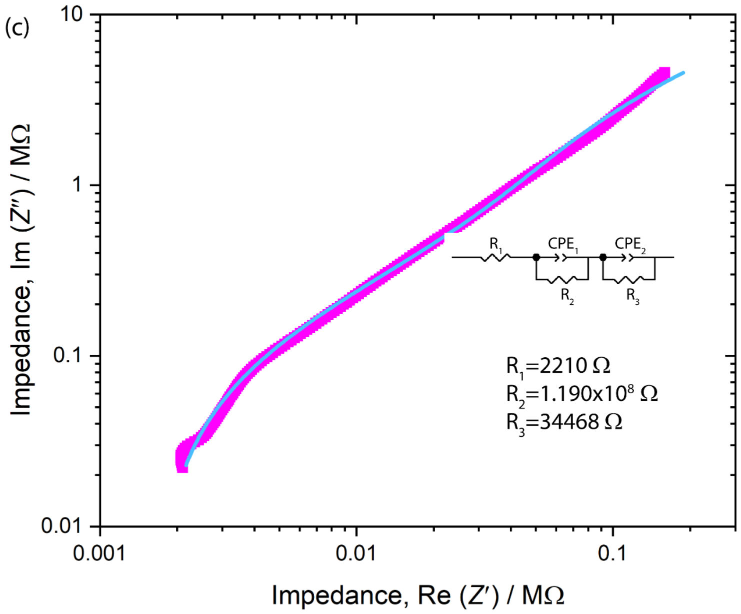

(c)
R1=2210 Ω
R2=1.190x10^8 Ω
R3=34468 Ω
Impedance, Im (Z″) / MΩ
Impedance, Re (Z′) / MΩ

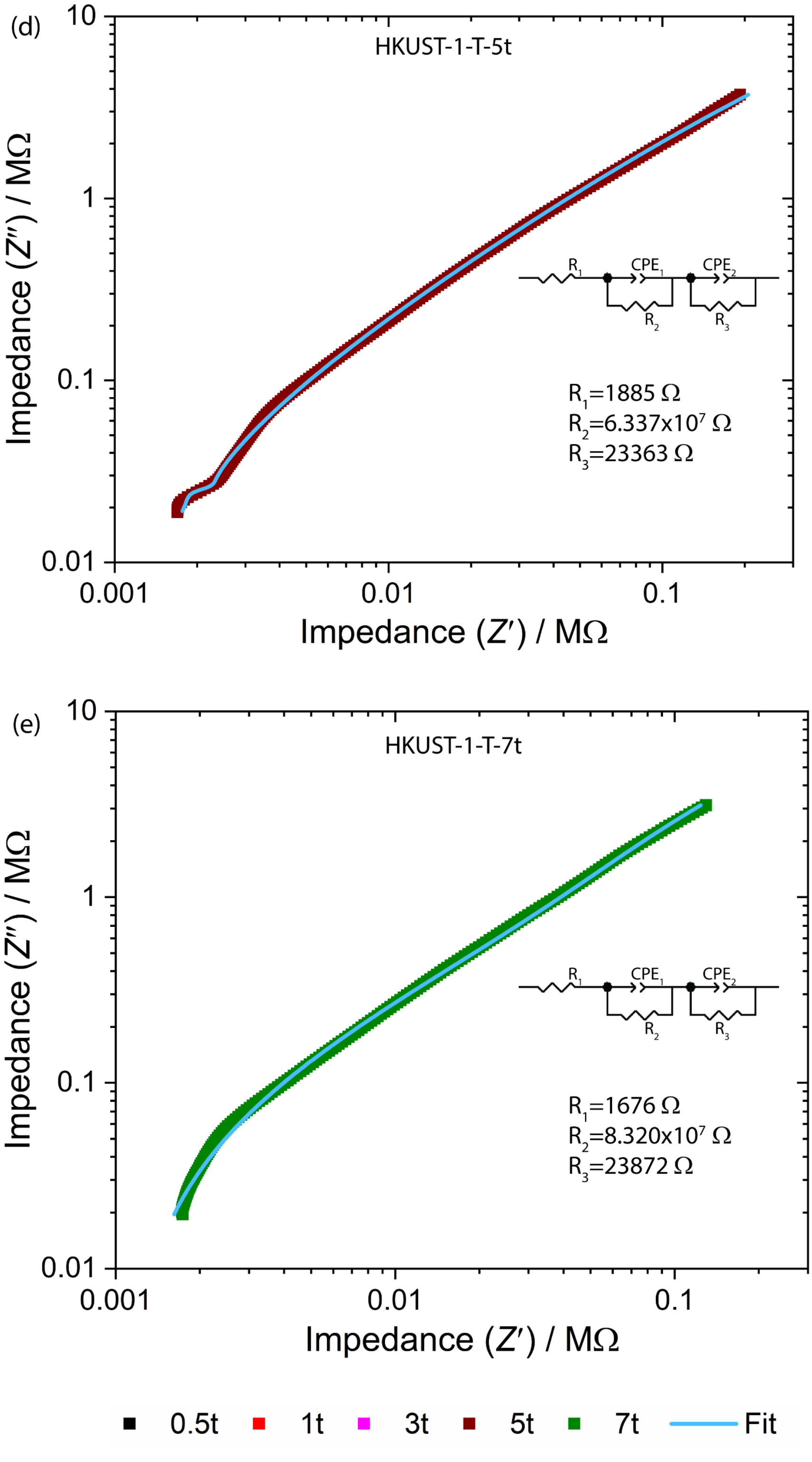

Figure 25: Impedance plot of real impedance vs imaginary impedance with the equivalent circuit at 20 °C for HKUST-1-T: (a) 0.5 ton, (b) 1 ton, (c) 3 ton, (d) 5 ton and (e) 7 ton.

Table S1: Conductivity of HKUST-1 pellets calculated by fitting the equivalent circuit in the impedance data.

Sample designation		Conductivity (S cm^{-1})		
	HKUST-1-S			HKUST-1-T
	20 °C	100 °C	20 °C	100 °C
0.5t	1.65×10^{-8}	2.79×10^{-8}	2.51×10^{-8}	1.16×10^{-7}
1t	2.51×10^{-8}	2.23×10^{-8}	5.63×10^{-8}	1.39×10^{-7}
3t	2.59×10^{-8}	2.32×10^{-8}	8.40×10^{-8}	2.05×10^{-7}
5t	2.16×10^{-8}	2.98×10^{-8}	1.58×10^{-7}	4.39×10^{-7}
7t	4.21×10^{-8}	4.25×10^{-8}	1.020×10^{-7}	5.37×10^{-7}